ICE, CLOUD, and Land Elevation Satellite-2 (ICESat-2) Project

Algorithm Theoretical Basis Document (ATBD) For

Land-Ice Along-Track Products Part 2:

Land-ice H(t)/ATL11

**Prepared By: Benjamin Smith, Suzanne Dickinson
Kaitlin Harbeck, Tom Neumann, David Hancock, Jeffery Lee, Benjamin Jelly**

**Goddard Space Flight Center
Greenbelt, Maryland**

**National Aeronautics and
Space Administration**

30 **Abstract**

31

32   **CM Foreword**

33   This document is an Ice, Cloud, and Land Elevation Satellite-2 (ICESat-2) Project Science
34   Office controlled document. Changes to this document require prior approval of the Science
35   Development Team ATBD Lead or designee. Proposed changes shall be submitted in the
36   ICESat-II Management Information System (MIS) via a Signature Controlled Request (SCoRe),
37   along with supportive material justifying the proposed change.
38   In this document, a requirement is identified by "shall," a good practice by "should," permission
39   by "may" or "can," expectation by "will," and descriptive material by "is."
40   Questions or comments concerning this document should be addressed to:
41   ICESat-2 Project Science Office
42   Mail Stop 615
43   Goddard Space Flight Center
44   Greenbelt, Maryland 20771
45

46 **Preface**

47
48 This document is the Algorithm Theoretical Basis Document for the TBD processing to be
49 implemented at the ICESat-2 Science Investigator-led Processing System (SIPS). The SIPS
50 supports the ATLAS (Advance Topographic Laser Altimeter System) instrument on the ICESat-
51 2 Spacecraft and encompasses the ATLAS Science Algorithm Software (ASAS) and the
52 Scheduling and Data Management System (SDMS). The science algorithm software will produce
53 Level 0 through Level 4 standard data products as well as the associated product quality
54 assessments and metadata information.
55 The ICESat-2 Science Development Team, in support of the ICESat-2 Project Science Office
56 (PSO), assumes responsibility for this document and updates it, as required, as algorithms are
57 refined or to meet the needs of the ICESat-2 SIPS. Reviews of this document are performed
58 when appropriate and as needed updates to this document are made. Changes to this document
59 will be made by complete revision.
60 Changes to this document require prior approval of the Change Authority listed on the signature
61 page. Proposed changes shall be submitted to the ICESat-2 PSO, along with supportive material
62 justifying the proposed change.
63 Questions or comments concerning this document should be addressed to:
64 Thorsten Markus, ICESat-2 Project Scientist
65 Mail Stop 615
66 Goddard Space Flight Center
67 Greenbelt, Maryland 20771
68

69   **Review/Approval Page**

Prepared by:

Benjamin Smith
Principal Researcher
University of Washington
Applied Physics Lab Polar Science Center
1013 NE 40th Street
Box 355640
Seattle, WA 98105

Reviewed by:

Shane Grigsby   *Ellen Enderlin*
Postdoctoral Scholar   *Assistant Professor*
Colorado School of Mines   *Department of Geosciences*
Department of Geophysics   *Boise State University*

          Approved by:

          Tom Neumann
          Project Scientist
          Code 615

70
71   ***** Signatures are available on-line at:** https:// /icesatiimis.gsfc.nasa.gov *******
72

73   **Change History Log**

Revision Level	Description of Change	SCoRe No.	Date Approved
1.0	Initial Release		
1.1	Changes for release 002. Calculate all crossovers (including near 88 S), determine the center of the y_atc search from the median of unique pair center locations.		
1.2	Changes for release 003. Add geoid and dem parameters.		
1.3	Improved the description of the polynomial coefficient writing process		

Release Date 20 March 2021

74   **List of TBDs/TBRs**

Item No.	Location	Summary	Ind./Org.	Due Date

75

76 **Table of Contents**

130

131 **List of Figures**

132
133 <u>Figure</u>   <u>Page</u>

143

144 **List of Tables**

145

152

1.0   INTRODUCTION

This document describes the theoretical basis and implementation of the level-3b land-ice processing algorithm for ATL11, which provides time series of surface heights. The higher-level products, providing gridded height, and gridded height change will be described in supplements to this document available in early 2020.

ATL11 is based on the ICESat-2 ATL06 Land-ice Height product, which is described elsewhere(Smith and others, 2019a, Smith and others, 2019b). ATL06 provides height estimates for 40-meter overlapping surface segments, whose centers are spaced 20 meters along each of ICESat-2's RPTs (reference pair tracks), but displaced horizontally both relative to the RPT and relative to one another because of small (a few tens of meters or less) imprecisions in the satellite's control of the measurement locations on the ground. ATL11 provides heights corrected for these offsets between the reference tracks and the location of the ATLAS measurements. It is intended as an input for high-level products, ATL15 and ATL16, which will provide gridded estimates of ice-sheet height and height change, but also may be used alone, as a spatially-organized product that allows easy access to height-change information derived from ICESat-2.

ATL11 employs a technique which builds upon those previously used to measured short-term elevation changes using ICESat repeat-track data. Where surface slopes are small and the geophysical signals are large compared to background processes (i.e., ice plains and ice shelves), some studies have subtracted the mean from a collection of height measurements from the same repeat track to leave the rapidly-changing components associated with subglacial water motion (Fricker and others, 2007) or tidal flexure (Brunt and others, 2011). In regions where off-track surface slopes are not negligible, height changes can be recovered if the mean height and an estimate of the surface slope (Smith and others, 2009) are subtracted from the data, although in these regions the degree to which the surface slope estimate and the elevation-change pattern are independent is challenging to quantify.

ICESat-2's ATL06 product provides both surface height and surface-slope information each time it overflies its reference tracks. The resulting data are similar to that from the scanning laser altimeters that have been deployed on aircraft in Greenland and Antarctica for two decades (cite), making algorithms originally developed for these instruments appropriate for use in interpreting ATLAS data. One example is the SERAC (Surface Elevation Reconstruction and Change Detection) algorithm (Schenk & Csatho, 2012) provides an integrated framework for the derivation of elevation change from altimetry data. In SERAC, polynomial surfaces are fit to collections of altimetry data in small (< 1 km) patches, and these surfaces are used to correct the data for sub-kilometer surface topography. The residuals to the surface then give the pattern of elevation change, and polynomial fits to the residuals as a function of time give the long-term pattern of elevation change. The ATL11 algorithm is similar to SERAC, except that (1) polynomial fit correction is formulated somewhat differently, so that the ATL11 correction gives the surface height at the fit center, not the height residual, and (2) ATL11 does not include a polynomial fit with respect to time.

194 **2.0   BACKGROUND INFORMATION AND OVERVIEW**

195   This section provides a conceptual description of ICESat-2's ice-sheet height measurements and
196   gives a brief description of the derived products.

197   **2.1   Background**

198   The primary goal of the ICESat-2 mission is to estimate mass-balance rates for the Earth's ice
199   sheets. An important step in this process is the calculation of height change at specific locations
200   on the ice sheets. In an ideal world, a satellite altimeter would exactly measure the same point
201   on the earth on each cycle of its orbit. However, there are limitations in a spacecraft's ability to
202   exactly repeat the same orbit and to point to the same location. These capabilities are greatly
203   improving with technological advances but still have limits that need to be accounted for when
204   estimating precise elevation changes from satellite altimetry data. The first ICESat mission
205   allowed estimates of longer-term elevation rates using along-track differencing, because
206   ICESat's relatively precise (50-150-m) pointing accuracy, precise (4-15 m) geolocation
207   accuracy, and small (35-70-m) footprints allowed it to resolve small-scale ice-sheet topography.
208   However, because ICESat had a single-beam instrument, its repeat-track measurements were
209   reliable only for measuring the mean rate of elevation change, because shorter-term height
210   differences could be influenced by the horizontal dispersion of tracks on a sloping surface.
211   ICESat-2 makes repeat measurements over a set of 1387 reference ground tracks (RGTs),
212   completing a *cycle* over all of these tracks every 91 days.   ICESat-2's ATLAS instrument
213   employs a split-beam design, where each laser pulse is divided six separate beams. The beams
214   are organized into three *beam pairs*, with each separated from its neighbors by 3.3 km (**Figure
215   2-1**), each pair following a reference pair track (RPT) that is parallel to the RGT.   The beams
216   within each pair separated by 90 m, which means that each cycle's measurement over an RPT
217   can determine the surface slope independently, and a height difference can be derived from
218   any two measurements of an RPT. The 90-m spacing between the laser beams in each pair
219   is equal to twice the required RMS accuracy with which ICESat-2 can be pointed at its RPTs,
220   which means that for most, but not all, repeat measurements of a given RPT, the pairs of
221   beams will overlap one another. To obtain a record of elevation change from the collection
222   of paired measurements on each RPT, some correction is still necessary to account for the
223   effects of small-scale surface topography around the RPT in the ATL06 surface heights that
224   appear as a result of this non-exact pointing. ATL11 uses a polynomial fit to the ATL06
225   measurements to correct for small-scale topography effects on surface heights that result
226   from this non-exact pointing.
227   The accuracy of ICESat-2 measurements depends on the thickness of clouds between the
228   satellite and the surface, on the reflectance, slope, and roughness of the surface, and on
229   background noise rate which, in turn, depends on the intensity of solar illumination of the
230   surface and the surface reflectance. It also varies from laser beam to beam, because in each
231   of ICESat-2's beam pairs one beam (the "strong beam") has approximately four times the
232   signal strength of the other (the "weak beam"). Parameters on the ATL06 product allow
233   estimation of errors in each measurement, and allow filtering of most measurements with
234   large errors due to misidentification of clouds or noise as surface returns (blunders), but to

2

235 enable higher precision surface change estimates, ATL11 implements further self-
236 consistency checks that further reduce the effects of errors and blunders.
237

Figure 2-1. ICESat-2 repeat-track schematic
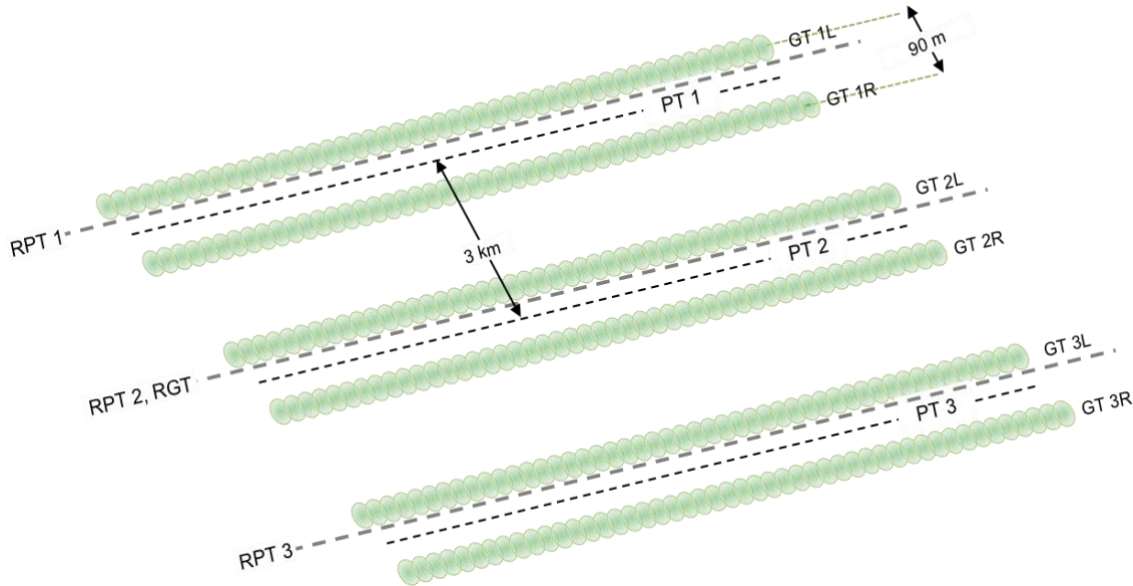
 Schematic drawing showing the pattern made by ATLAS's 6-beam configuration on the ground, for a
track running from lower left to upper right. The 6 beams are grouped into 3 beam pairs with a
separation between beams within a pair of 90m and a separation between beam pairs of 3.3 km. The
RPTs (Reference Pair Tracks, heavily dashed lines in gray) are defined in advance of launch; the central
RPT follows the RGT (Reference Ground Track, matching the nadir track of the predicted orbit). The
Ground Tracks are the tracks actually measured by ATLAS (GT1L, GT1R, etc., shown by green
footprints). Measured Pair Tracks (PTs, smaller dashed lines in black) are defined by the centers of the
pairs of GTs, and deviate slightly from the RPTs because of inaccuracies in repeat-track pointing. The
separation of GTs in each pair in this figure is greatly exaggerated relative to the separation of the PTs.

238 **2.2   Elevation-correction Coordinate Systems**

239 We perform ATL11 calculations using the along-track coordinate system described in the
240 ATL06 ATBD (Smith and others, 2019b, Smith and others, 2019a). The along-track coordinate
241 is measured parallel to the RGT, starting at each RGT's origin at the equator. The across-track
242 coordinate is measured to the left of the RGT, so that the two horizontal basis vectors and the
243 local vertical vector form a right-handed coordinate system.

244 **2.3   Terminology:**

245 Some of the terms that we will use in describing the ATL11 fitting process and the data
246 contributing are:

247 *RPT*: Reference pair track
248 *Cycle:* ICESat-2 has 1387 distinct reference ground tracks, which its orbit covers every 91 days.
249 One repeat measurement of these reference ground tracks constitutes a cycle.
250 *ATL06 segment:* A 40-meter segment fit to a collection of ATL03 photon-event data, as
251 described in the ATL06 ATBD
252 *ATL06 pair*: Two ATL06 segments from the same cycle with the same *segment_id*. By
253 construction, both segments in the ATL06 pair have the same along-track coordinate, and are
254 separated by the beam-to-beam spacing (approximately 90 m) in the across-track direction
255 *ATL11 RPT point*: The expected location of each ATL11 point on the RPT, equivalent to the
256 beginning of every third geosegment on the RPT, or the center of every third ATL06 segment.
257 *ATL11 reference point*: an *ATL11 RPT point* shifted in the across-track direction to better match
258 the geometry of the available ATL06 data.
259 *ATL11 fit:* The data and parameters associated with a single ATL11 reference point. This
260 includes corrected heights from all available cycles
261
262 ATL11 calculates elevations and elevation differences based on collections of segments from the
263 same beam pair but from different cycles. ATL11 is posted every 60 m, which corresponds to
264 every third ATL06 *segment_id*, and includes ATL06 segments spanning three segments before
265 and after the central segment, so that the ATL11 uses data that span 120 m in the along-track
266 direction. ATL11 data are centered on *reference points*, which has the same along-track
267 coordinate as its central ATL06 segment, but is displaced in the across-track direction to better
268 match the locations of the ATL06 measurements from all of the cycles present (see section
269 3.1.3).

Figure 2-2. ATL06 data for an ATL11 reference point
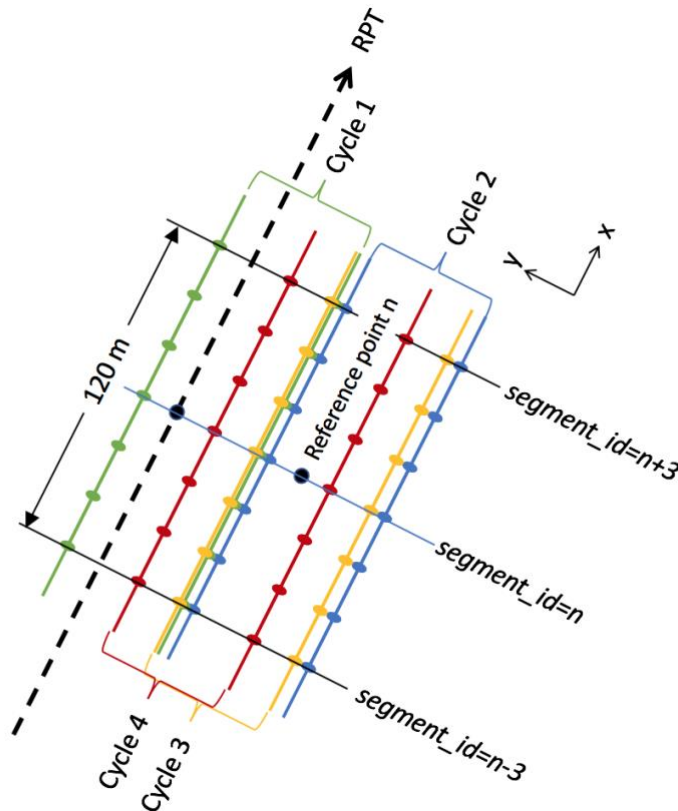
Schematic of ATL06 data for an ATL11 reference point centered on segment n, based on data from four cycles. The segment centers span 120 m in the along-track data, and the cycles are randomly displaced from the RPT in the across-track direction. The reference point has an along-track location that matches that of segment n, and an across-track position chosen to match the displacements of the cycles.

270

2.4   Repeat and non-repeat cycles in the ICESat-2 mission

271

272 In the early part of the ICESat-2 mission, an error in the configuration of the start trackers
273 prevented the instrument from pointing precisely at the RGTs. As a result, all data from cycles 1
274 and 2 were measured between one and two kilometers away from the RGTs, with offsets that
275 varied in time and as a function of latitude. The measurements from cycles 1 and 2 still give
276 high-precision measurements of surface height, but repeat-track measurements from ICESat-2
277 begin during cycle 3, in April of 2019. ATL11 files will be generated for ATL06 granules from
278 cycles 1 and 2, but these will contain only one cycle of data, plus crossovers, because the
279 measurements from these cycles (which are displaced from the RPTs by several kilometers) will
280 not be repeated. We expect the measurements from cycles 1 and 2 to be useful as a reduced-
281 resolution (compared to ATL06) mapping of the ice sheet, which may prove useful in DEM
282 generation and in comparisons with other altimetry missions. For cycles 3 and after, each
283 ATL11 granule will contain all available cycles for each RGT (i.e. from cycle 3 onwards), and
284 will contain crossovers between the repeat cycles and cycles 1 and 2.

5

285 Outside the polar regions, ICESat-2 is pointed to minimize gaps between repeat measurements,
286 and so does not make repeat measurements over its ground tracks. ATL11 is   only calculated
287 within the repeat-pointing mask (see Figure ???), which covers areas poleward of 60°N and
288 60°S.
289

2.5 Physical Basis of Measurements / Summary of Processing

291 Surface slopes on the Antarctic and Greenland ice sheets are generally small, with magnitudes
292 less than two degrees over 99% of Antarctica's area. Smaller-scale (0.5-3 km) undulations,
293 generated by ice flow over hilly or mountainous terrain may have amplitudes of up to a few
294 degrees. Although we expect that the surface height will change over time, slopes and locations
295 of these smaller-scale undulation are likely controlled by underlying topography and should
296 remain essentially constant over periods of time comparable with the expected 3-7 duration of
297 the ICESat-2 mission. This allows us to use estimates of ice-sheet surface shape derived from
298 data spanning the full mission to correct for small (<130-m) differences in measurement
299 locations between repeat measurements of the same RPT, to produce records of height change
300 for specific locations. To account for changes in the ice-sheet surface slope associated with
301 gradients in thinning, we also solve for the rate of surface-slope change, when sufficient data are
302 available. Further, we can use the surface slope estimates in ATL06 to determine whether
303 different sets of measurements for the same fit center are self-consistent: We can assume that if
304 an ATL06 segment shows a slope significantly different from others measured near the same
305 reference point it likely is in error. The combination of parameters from ATL06 and these self-
306 consistency checks allows us to generate time series based on the highest-quality measurements
307 for each reference point, and our reference surface calculation lets us correct for small-scale
308 topography and to estimate error magnitudes in the corrected data.

2.5.1 Choices of product dimensions

310 We have chosen a set of dimensions for the ATL11 fitting process with the goal of creating a
311 product that is conveniently sized for analysis of elevation changes, while still capturing the
312 details of elevation change in outlet glaciers. The assumption that ice-sheet surface can be
313 approximated by a low-degree polynomial becomes untenable as data from larger and larger
314 areas are included in the calculation; therefore we use data from the smallest feasible area to
315 define our reference surface, while still including enough data to reduce the sampling error in the
316 data and to allow for the possibility that at least one or two will encounter a flat surface, which
317 greatly improves the chances that each cycle will be able to measure surface comparable to one
318 another. Each ATL11 point uses data from an area up to 120 m in the along-track direction by
319 up to 130 m in the across-track direction. We have chosen the cross-track search distance
320 (L_{search_XT}) to be 65 m, approximately equal to half the beam spacing, plus three times the
321 observed 6.5 m standard deviation of the across-track pointing accuracy for cycles 3 and 4 in
322 Antarctica. We chose the across-track search distance (L_{search_AT}) to be 60 m, approximately
323 equal to L_{search_XT}, so that the full L_{search_AT} search window spans three ATL06 segments before
324 and after the central segment for each reference point. The resulting along-track resolution is

6

325 around one third that of ATL06, but still allows 6-7 distinct elevation-change samples across a
326 small (1-km) outlet glacier.

327 **2.6   Product coverage**

Figure 2-3. Potential ATL11 coverage

Maximum number of valid repeat measurements from an ATL11 file for each 10-km segment of pair track 2.
Yellower colors indicate areas where ICESat-2 has systematically pointed at the RGTs.
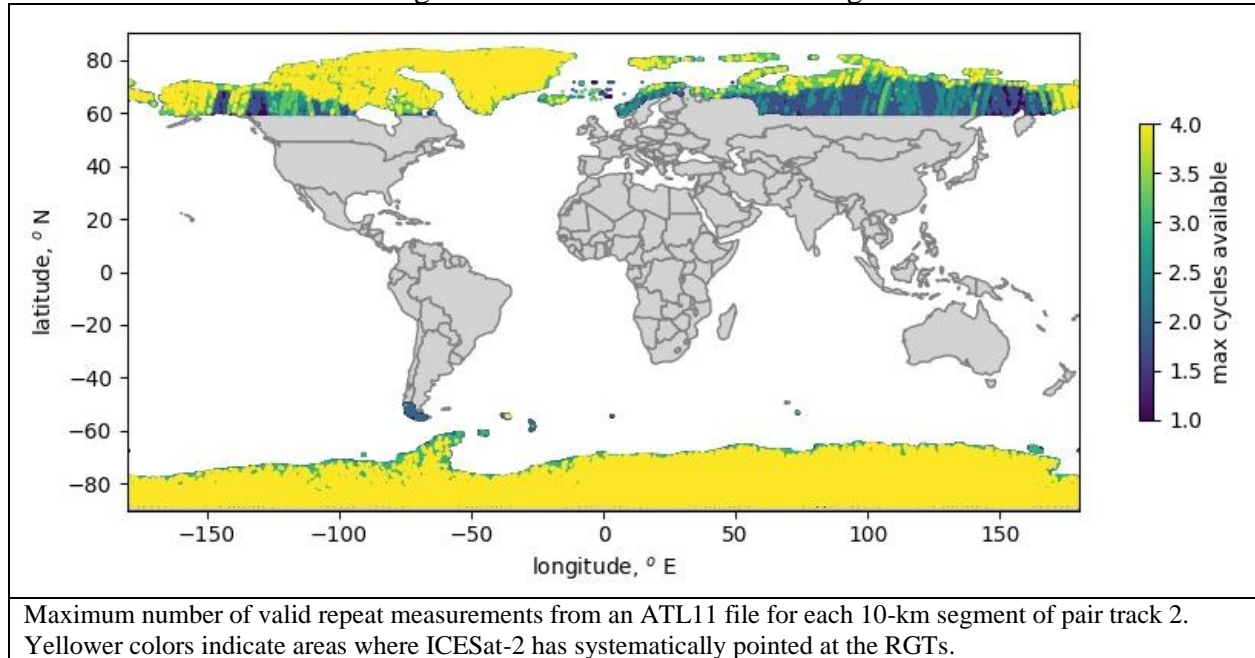
328 Over the vegetated parts of the Earth, ICESat-2 makes spatially dense measurements, measuring
329 tracks parallel to the reference tracks in a strategy that will eventually measure global vegetation
330 with a track-to-track spacing better than 1 km. Because ATL11 relies upon repeat measurements
331 over reference tracks to allow the calculation of its reference surfaces, ATL11 is generated for
332 ICESat-2 subregions 3-5 and 10-12 (global coverage, north and south of 60 degrees). Repeat
333 measurements are limited to Antarctica, Greenland, and the High Arctic islands (Figure 2-3),
334 although in other areas the fill-in strategy developed for vegetation measurements allows some
335 repeat measurements. In regions where ICESat-2 was not pointed to the repeat track, most
336 ATL11 reference points will provide one measurement close to the RPT. Crossover data are
337 available for many of these points, though their distribution in time is not regular. A future
338 update to the product may provide crossover measurements for lower-latitude areas, but the
339 current product format is not designed to allow this.

340 **3.0   ALGORITHM THEORY: DERIVATION OF LAND ICE H (T)/ATL11 (L3B)**

341 In this section, we describe in detail the algorithms used in calculating the ATL11 land-ice
342 parameters. This product is intended to provide time series of surface heights for land-ice and
343 ice-shelf locations where ICESat-2 operates in repeat-track mode (*i.e*. for polar ice), along with
344 parameters useful in determining whether each height estimate is valid or a result of a variety of
345 potential errors (see ATL06 ATBD, section 1).
346 ATL11 height estimates are generated by correcting ATL06 height measurements for the
347 combined effects of short-scale (40-120-m) surface topography around the fit centers and small
348 (up to 130-m) horizontal offsets between repeat measurements. We fit a polynomial reference
349 surface to height measurements from different cycles as a function of horizontal coordinates
350 around the fit centers, and use this polynomial surface to correct the height measurements to the
351 fit center. The resulting values reflect the time history of surface heights at the reference points,
352 with minimal contributions from small-scale local topography.
353 In this algorithm, for a set of reference points spaced every 60 meters along each RPT (centered
354 on every third segment center), we consider all ATL06 segments with centers within 60 m along-
355 track and 65 m across-track of the reference point, so that each ATL11 fit contains as many as
356 seven distinct along-track segments from each laser beam and cycle. We select a subset of these
357 segments with consistent ATL06 slope estimates and small error estimates, and use these
358 segments to define a time-variable surface height and a polynomial surface-shape model. We
359 then use the surface-shape model to calculate corrected heights for the segments from cycles not
360 included in the initial subset.   We propagate errors for each of these steps to give formal errors
361 estimates that take into account the sampling error from ATL06, and propagate the geolocation
362 errors with the slope of the surface-shape model to give an estimate of systematic errors in the
363 height estimates.

Figure 3-1. ATL11 fitting schematic

8
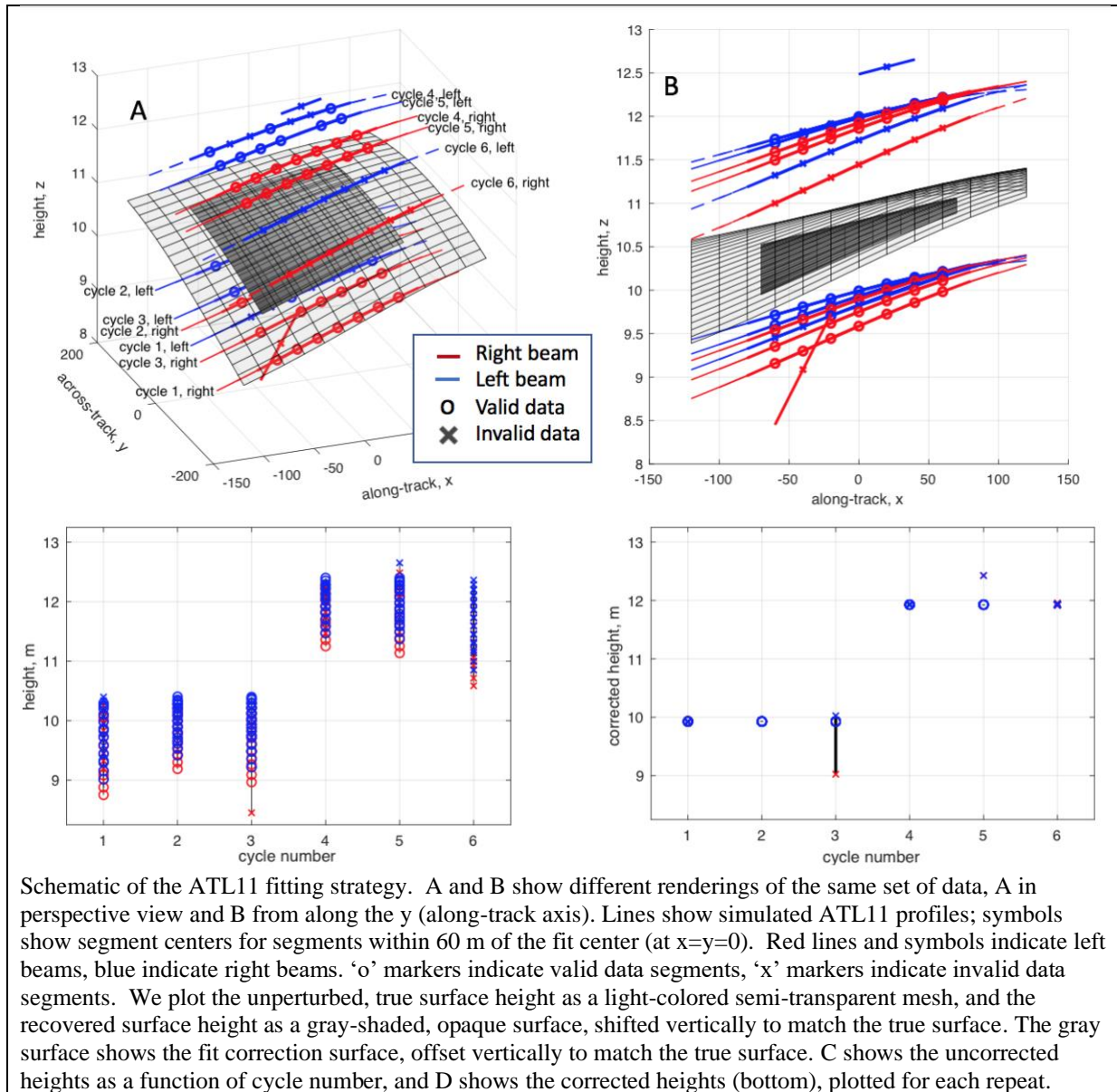
Schematic of the ATL11 fitting strategy. A and B show different renderings of the same set of data, A in perspective view and B from along the y (along-track axis). Lines show simulated ATL11 profiles; symbols show segment centers for segments within 60 m of the fit center (at x=y=0). Red lines and symbols indicate left beams, blue indicate right beams. 'o' markers indicate valid data segments, 'x' markers indicate invalid data segments. We plot the unperturbed, true surface height as a light-colored semi-transparent mesh, and the recovered surface height as a gray-shaded, opaque surface, shifted vertically to match the true surface. The gray surface shows the fit correction surface, offset vertically to match the true surface. C shows the uncorrected heights as a function of cycle number, and D shows the corrected heights (bottom), plotted for each repeat.

364
365 Figure 3-1 shows a schematic diagram of the fitting process. In this example, we show simulated
366 ATL06 height measurements for six 91-day orbital cycles over a smooth ice-sheet surface
367 (transparent grid). Between cycles 3 and 4, the surface height has risen by 2 m. Two of the
368 segments contain errors: The weak beam for one segment from repeat 3 is displaced downward
369 and has an abnormal apparent slope in the *x* direction, and one segment from repeat 5 is
370 displaced upwards, so that its pair has an abnormal apparent slope in the *y* direction. Segments
371 falling within the across and along-track windows of the reference point (at *x*=*y*=0 in this plot)
372 are selected, and fit with a polynomial reference surface (shown in gray). When plotted as a
373 function of cycle number (panel C), the measured heights show considerable scatter but when
374 corrected to the reference surface (panel D), each cycle shows a consistent height, and the
375 segments with errors are clearly distinct from the accurate measurements.

9

376 **3.1   Input data editing**

377 Each ATL06 measurement includes location estimates, along- and across-track slope estimates,
378 and PE (Photon-Event)-height misfit estimates. To calculate the reference surface using the most
379 reliable subset of available data, we perform tests on the surface-slope estimates and error
380 statistics from each ATL06-pair to select a self-consistent set of data. These tests determine
381 whether each pair of measurements is *valid* and can be used in the reference-shape calculation or
382 is *invalid*. Segments from invalid pairs may be used in elevation-change calculations, but not in
383 the reference-shape calculation.
384 A complete flow chart of the data-selection process is shown in Figure 3-2, and the parameters
385 used to make these selections and their values are listed in Table 3-1.

386

387   **Table 3-1 Parameter Filters to determine the validity of segments for ATL11 estimates**

complex_surface_flag	Segment parameter	Filter strategy	Section
0	*ATL06_quality_summary*	*ATL06_quality_summary* =0 (indicates high-quality segments)	*3.1.1*
1	*SNR_significance*	*SNR_significance < 0.02* (indicates low probability of surface-detection blunders)	*3.1.1*
0 or 1	Along-track differences	Minimum height difference between the endpoints of a segment and the middles of its neighbors must be < 2 m (for smooth surfaces) or < 10 m (for complex surfaces)	*3.1.1*
0 or 1	*h_li_sigma*	$h_li_sigma < $ max(0.05, 3*median(h_li_sigma))	3.1.1
0 or 1	Along-track slope	$|r\_slope\_x| < 3$ *slope_tolerance_x*	3.1.2
0 or 1	Across-track slope	$|r\_slope\_y| < 3$ *slope_tolerance_y*	3.1.2
0 or 1	Segment location	$|x\_atc\text{-}x_0| < L\_search\_XT$ $|y\_atc\text{-}y_0| < L\_search\_AT$	3.1.3

Figure 3-2. Data selection

10
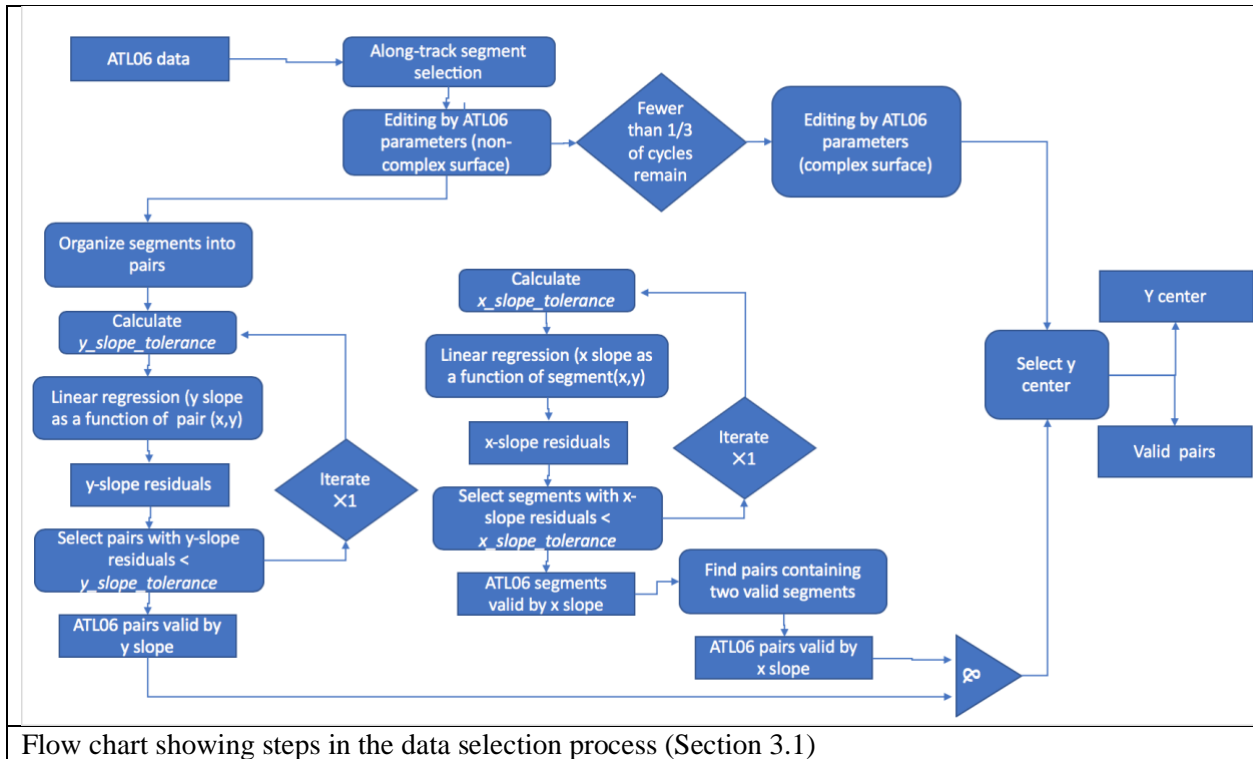
Flow chart showing steps in the data selection process (Section 3.1)

388

3.1.1 Input data editing using ATL06 parameters

390   For each reference point, we collect all ATL06 data from all available repeat cycles that have
391   *segment_id* values within ±3 of the reference point (inclusive) and that are on the same *rgt* and
392   pair track as the reference point. The *segment_id* criterion ensures that the segment centers are
393   within ±60 m of the reference point in the along-track direction. We next check that the ATL06
394   data are close to the pre-defined reference track, by rejecting all ATL06 segments that are more
395   than 500 m away from the nominal pair across-track coordinates (-3200, 0, and 3200 meters for
396   right, center, and left pairs, respectively). This removes data that were intentionally or
397   accidentally collected with ATLAS pointed off nadir (i.e. for calibration scan maneuvers).
398   ATL06 contains some segments with signal-finding blunders (Smith et al., 2019). To avoid
399   having these erroneous segments contaminate ATL11, we filter using one of two sets of tests,
400   depending on surface roughness. We identify high-quality ATL06 segments, using parameters
401   that depend on whether the surface is identified as smooth or rough, as follows:
402   1) For smooth ice-sheet surfaces, we use the ATL06 *ATL06_quality_summary* parameter,
403   combined with a measure of along-track elevation consistency, *at_min_dh*, that is calculated as
404   part of ATL11. *ATL06_quality_summary* is based on the spread of the residuals for each
405   segment, the along-track surface slope, the estimated error, and the signal strength. Zero values
406   indicate that no error has been found. We define the along-track consistency parameter
407   *at_min_dh* as the minimum absolute difference between the heights of the endpoints of each
408   segment and the center heights of the previous and subsequent segments. Its value will be small
409   if a segment's height and slope are consistent with at least one of its neighbors. For smooth

11

410 surfaces, we require that the *at_min_dh* values be less than 2 m. Over smooth ice-sheet surfaces,
411 the 2-m threshold eliminates most blunders without eliminating a substantial number of high-
412 quality data points.
413 2) For rough, crevassed surfaces, the smooth-ice strategy may not identify a sufficient number of
414 pairs for ATL11 processing to continue. If fewer than one third of the original cycles remain
415 after the smooth-surface criteria are applied, we relax our criteria, using the signal-to-noise ratio
416 (based on the ATL06 *segment_stats/snr_significance* parameter) to select the pairs to include in
417 the fit, and require that the *at_min_dh* values be less than 10 m. If we relax the criteria in this
418 way, we mark the reference point as having a complex surface using the
419 *ref_surf/complex_surface_flag,* which limits the degree of the polynomial used in the reference
420 surface fitting to 0 or 1 in each direction.
421 For either smooth or rough surfaces, we perform an additional check using the magnitude of
422 *h_li_sigma* for each segment. If any segment's value is larger than three times the maximum of
423 0.05 m and the median *h_li_sigma* for the valid segments for the current reference point, it is
424 marked as invalid. The limiting 0.05 m value prevents this test from removing high-quality data
425 over smooth ice-sheet surfaces, where errors are usually small.
426 Each of these tests applies to values associated with ATL06 segments. When the tests are
427 complete, we check each ATL06 pair (*i.e.* two segments for the same along-track location from
428 the same cycle) and if either of its two segments has been marked as invalid, the entire pair is
429 marked as invalid.

430 **3.1.2 Input data editing by slope**

431 The segments selected in 3.1.1 may include some high-quality segments and some lower-quality
432 segments that were not successfully eliminated by the data-editing criteria. We expect that the
433 ATL06 slope fields (*dh_fit_dx,* and *dh_fit_dy*) for the higher-quality data should reflect the
434 shape of an ice-sheet surface with a spatially consistent surface slope around each reference
435 point, but that at least some of lower-quality data should have slope fields that outliers relative to
436 this consistent surface slope. In this step, we assume that the slope may vary linearly in *x* and *y*,
437 and so use residuals between the slope values and a regression of the slope values against *x* and *y*
438 to identify the data with inconsistent slope values. The data with large residuals are marked as
439 *invalid.*
440 Starting with valid pairs from 3.2.1*,* we first perform a linear regression between the *y* slopes of
441 the pairs and the pair-center *x* and *y* positions. The residuals to this regression define one
442 *y_slope_residual* for each pair. We compare these residuals against a *y_slope_tolerance:*

$$y\_slope\_tolerance = max(0.01, 3\ median\ (dh\_fit\_dy\_sigma), 3\ RDE \qquad 1$$
$$(y\_slope\_residuals))$$

443 Here RDE is the Robust Difference Estimator, equal to half the difference between the 16th and
444 84th percentiles of a distribution, and the minimum value of 0.01 ensures that this test does not
445 remove high-quality segments in regions where the residuals are very consistent. If any pairs
446 have a *y_slope_residual* greater than *y_slope_tolerance,* we remove them from the group of valid
447 pairs, then repeat the regression, recalculate *y_slope_tolerance,* and retest the remaining pairs.
448 We then return to the pairs marked as *valid* from 3.1.1, and perform a linear regression between
449 the *x* slopes of the segments within the pairs and the segment-center *x* and *y* positions. The

450 residuals to this regression define one *x_slope_residual* for each segment. We compare these
451 residuals against an *x_slope_tolerance,* calculated in the same way as (1), except using segment *x*
452 slopes and residuals instead of pair *y* slopes. As with the *y* regression, we repeat this procedure
453 once if any segments are eliminated in the first round.
454 After both the *x* and *y* regression procedures are complete, each pair of segments is marked as
455 *valid* if both of its *x* residuals are smaller than *slope_tolerance_x* and its *y* residual is smaller than
456 *slope_tolerance_y.*

457 3.1.3 Spatial data editing

458 The data included in the reference-surface fit fall in a "window" defined by a $2L_{search\ XT}$ by
459 $2L_{search\ AT}$ rectangle, centered on each reference point. Because the across-track location of the
460 repeat measurements for each reference point are determined by the errors in the repeat track
461 pointing of ATLAS, a data selection window centered on the RPT in the *y* direction will not
462 necessarily capture all of the available cycles of data. To improve the overlap between the
463 window and the data, we shift the reference point in the *y* direction so that the window includes
464 as many valid beam pairs as possible. We make this selection after the parameter-based (3.1.1)
465 and slope-based (3.1.2) editing steps because we want to maximize the number high-quality pairs
466 included, without letting the locations of low-quality segments influence our choice of the
467 reference-point shift.
468 We select the across-track offset for each reference point by searching a range of offset values, δ,
469 around the RPT to maximize the following metric:

$$M(\delta) = [number\ of\ unique\ valid\ pairs\ entirely\ contained\ in\ \delta \pm L_{search\ XT}]^2 + [number\ of\ unpaired\ segments\ contained\ in\ \delta \pm L_{search\ XT}]/100$$

470 Maximizing this metric allows the maximum number of pairs with two valid segments to be
471 included in the fit, while also maximizing the number of segments included close to the center of
472 the fit. If multiple values of δ have the same M value we choose the median of those δ values.
473 The across-track coordinate of the adjusted reference point is then *y₀+δ_max,* where *y₀* is the
474 across-track coordinate of the unperturbed reference point. After this adjustment, the segments
475 in pairs that are contained entirely in the across-track interval $\delta \pm L_{search\ XT}$ are identified as
476 *valid* based on the spatial search.
477 The location of the adjusted reference point is reported in the data group for each pair track, with
478 corresponding local coordinates in the *ref_surf* subgroup: */ptx/ref_surf/x_atc, /ptx/ref_surf/y_atc.*
479

480 3.2   Reference-Surface Shape Correction

481 To calculate the reference-surface shape correction, we construct the background surface shape
482 from valid segments selected during 3.1 and 3.2, using a least-squares inversion that separates
483 surface-shape information from elevation-change information. This produces surface shape-
484 corrected height estimates for cycles containing at least one valid pair, and a surface-shape
485 model that we use in later steps (3.4, 3.6) to calculate corrected heights for cycles that contain no
486 valid pairs and to calculate corrected heights for crossing tracks.

3.2.1 Reference-surface shape inversion

487

488 The reference-shape inversion solves for a reference surface and a set of corrected-height values
489 that represent the time-varying surface height at the reference point. The inversion involves
490 three matrices:
491 (*i*): a polynomial surface shape matrix, **S**, that describes the functional basis for the spatial part of
492 the inversion:

$$\mathbf{S} = \left[\left(\frac{x - x_0}{l_0}\right)^p \left(\frac{y - y_0}{l_0}\right)^q \right] \qquad\qquad 3$$

493 Here x_0 and y_0 are equal to the along-track coordinates of the adjusted reference point,
494 */ptx/ref_surf/x_atc* and */ptx/ref_surf/y_atc*, respectively. **S** has one column for each permutation
495 of *p* and *q* between zero and the degree of the surface polynomial in each dimension, but does
496 not include a *p=q=0* term. The degree is chosen to be no more than 3 (in the along-track
497 direction) or 2 (in the across-track direction), and to be no more than the number of distinct pair-
498 center y values (in the across-track direction) or more than 1 less than the number of distinct x
499 values (in the along-track direction) in any cycle, with distinct values defined at a resolution of
500 20 m in each direction. The scaling factor, l_0, ensures that the components of S are on the order
501 of 1, which improves the numerical accuracy of the computation. We set l_0=100 m, to
502 approximately match the intra-pair beam spacing.
503 (ii): a matrix that encodes the repeat structure of the data, that accounts for the height-change
504 component of the inversion:

$$\mathbf{D} = [\delta(i, 1), \delta(i, 2), \quad ..., \delta(i, N)] \qquad\qquad 4$$

505 Here δ is the delta function, equal to 1 when its arguments are equal, zero otherwise, and *i* is an
506 index that increments by one for each distinct cycle in the selected data.
507 (iii): a matrix that describes the linear rate of change in the surface slope over the course of the
508 mission:

$$\mathbf{S}_t = \left[\left(\frac{x - x_0}{l_0}\right) \left(\frac{t - t_0}{\tau}\right), \left(\frac{y - y_0}{l_0}\right) \left(\frac{t - t_0}{\tau}\right) \right] \qquad\qquad 5$$

509 Here t_0 is equal to *slope_change_t0*, the mid-point of the mission at the time that ATL11 is
510 generated, halfway between start repeat track pointing (the beginning of cycle 3) and either the
511 end of the mission or the processing time (*slope_change_t0 is an attribute of each ATL11*
512 *file*). This implies that on average, $(t - t_0)$ will have a zero mean. The time-scaling factor, τ, is
513 equal to one year (86400*365.25 seconds). This component will only be included in ATL11
514 once eight complete cycles of data are available on the RGTs (after cycle 10 of the mission).
515 The surface shape, slope change, and height time series are estimated by forming a composite
516 design matrix, **G**, where

$$\mathbf{G} = [\mathbf{S}\ \mathbf{S}_t\ \mathbf{D}], \qquad\qquad 6$$

517 and a covariance matrix, **C**, containing the squares of the segment-height error estimates on its
518 diagonal. The surface-shape polynomial and the height changes are found:

$$[\mathbf{s}, \mathbf{s}_t, \mathbf{z}_c] = \mathbf{G}^{-\mathbf{g}}\mathbf{z}$$
$$\text{where} \qquad\qquad 7$$
$$\mathbf{G}^{-\mathbf{g}} = [\mathbf{G}^T\mathbf{C}^{-1}\mathbf{G}]^{-1}\mathbf{G}^T\mathbf{C}^{-1}$$

14

519   The notation $[]^{-1}$ designates the inverse of the quantity in brackets, and **z** is the vector of segment
520   heights.   The parameters derived in this fit are **s**, a vector of surface-shape polynomial
521   coefficients, $\mathbf{s}_t$, the mean rate of surface-slope change, and $\mathbf{z}_c$, a vector of corrected height values,
522   giving the height at (*lat₀, lon₀*) as inferred from the height measurements and the surface
523   polynomial. The matrix $\mathbf{G}^{-g}$ is the generalized inverse of **G**. The values of **s** are reported in the
524   *ref_surf/poly_ref_surf* parameter, as they are calculated from (6), with no correction made for the
525   scaling in (3). The values for the slope-change rates are reported in *ref_surf/slope_change_rate*,
526   after rescaling to units of *years⁻¹*.

3.2.2 Misfit analysis and iterative editing

528   If blunders remain in the data input to the reference-surface calculation, they can lead to
529   inaccurate reference surfaces. To help remove these blunders, we iterate the inversion procedure
530   in 3.2.1, eliminating outlying data points based on their residuals to the reference surface.
531   To determine whether outliers may be present, we calculate the chi-squared misfit between the
532   data and the fit surface based on the data covariance matrix and the residual vector, *r*:

$$\chi^2 = r^T \mathbf{C}^{-1} r \qquad\qquad 8$$

533   To determine whether this misfit statistic indicates consistency between the polynomial surface
534   and the data we use a P statistic, which gives the probability that the given χ value would be
535   obtained from a random Gaussian distribution of data points with a covariance matrix **C**. If the
536   probability is less than 0.025, we perform some further filtering/editing: we calculate the RDE of
537   the scaled residuals, eliminate any pairs containing a segment whose scaled residual magnitude is
538   larger than three times that value, and repeat the remaining segments.
539   After each iteration, any column of **G** that has a uniform value (i.e. all the values are the same) is
540   eliminated from the calculation, and the corresponding value of the left-hand side of equation 7
541   is set to zero. Likewise, if the inverse problem has become less than overdetermined (i.e., the
542   number of data is smaller than the number of unknown values they are constraining), the
543   polynomial columns of **G** are eliminated one by one until the number of data is greater than the
544   number of unknowns. Columns are eliminated in descending order of the sum of *x* and *y*
545   degrees, and when there is a tie between columns based on this criterion, the column with the
546   larger *y* degree is eliminated first.
547   This fitting procedure is continued until no further segments are eliminated. If more than three
548   complete cycles that passed the initial editing steps are eliminated in this way, the surface is
549   assumed to be too complex for a simple polynomial approximation, and we proceed as follows:
550   (*i*)   the fit and its statistics are reported based on the complete set of pairs that passed
551   the initial editing steps (valid pairs), using a planar (x degree = y_degree = 1) fit in *x* and *y*.
552   (*ii*) the *ref_surf/complex_surface_flag* is set to 1.
553   The misfit parameters are reported in the *ref_surf* group: The final chi-squared statistic is
554   reported as *ref_surf/misfit_chi2r*, equal to the chi-squared statistic divided by the number of
555   degrees of freedom in the solution; the final RMS of the scaled residuals is reported as
556   *ref_surf/misfit_rms*.

557 **3.3   Reference-shape Correction Error Estimates**

558   We first calculate the errors in the corrected surface heights for segments included in the
559   reference-surface fit. We form a second covariance matrix, $\mathbf{C}_1$, whose diagonal elements are the
560   maximum of the squares of the segment errors and $<r^2>$. We estimate the covariance matrix for
561   the height estimates:

$$\mathbf{C}_m = \mathbf{G}^{-g}\mathbf{C}_1\mathbf{G}^{-gT} \hspace{4cm} 9$$

562   The square roots of the diagonal values of $\mathbf{C}_m$ give the estimated errors in the surface-polynomial
563   and height estimates due to short-spatial-scale errors in the segment heights. If there are N_{coeff}
564   coefficients in the surface-shape polynomial, and $N_{shape\text{-}cycles}$ cycles included in the surface-shape
565   fit, then the first N_{coeff} diagonal elements of $\mathbf{C}_m$ give the square of the errors in the surface-shape
566   polynomial and the last $N_{shape\text{-}cycles}$ give the errors in the surface heights for the cycles included in
567   the fit. The portion of $\mathbf{C}_m$ that refers only to the surface shape and surface-shape change
568   components is $\mathbf{C}_{m,s}$.

569   **3.4   Calculating corrected height values for repeats with no selected pairs**

570   Once the surface polynomial has been established from the edited data set, corrected heights are
571   calculated for the unselected cycles (*i.e.* those from which all pairs were removed in the editing
572   steps): For the segments among these cycles, we form a new surface and slope-change design
573   matrix, $[\mathbf{S}, \mathbf{S}_t]$ and multiply it by $[\mathbf{s}, \mathbf{s}_t]$ to give the surface-shape correction:

$$\boldsymbol{z}_c = \boldsymbol{z} - [\mathbf{S}, \mathbf{S}_t][\mathbf{s}, \mathbf{s}_t] \hspace{4cm} 10$$

574   Here s is the surface-shape polynomial, and $\mathbf{s}_t$ is the slope-change-rate estimate. This gives up to
575   fourteen corrected-height values per unselected cycle. From among these, we select the segment
576   with the minimum error, as calculated in the next step.
577   The height errors for segments from cycles not included in the surface-shape fit are calculated:

$$\boldsymbol{\sigma}_{z,c}^2 = diag\big([\mathbf{S}, \mathbf{S}_t]\mathbf{C}_{m,s}[\mathbf{S}, \mathbf{S}_t]^T\big) + \sigma_z^2 \hspace{3cm} 11$$

578   Here $\boldsymbol{\sigma}_z$ is the error in the segment height, and $\boldsymbol{\sigma}_{z,c}$ is the error in the corrected height. The
579   results of these calculations give a height and a height error for each unselected segment. To
580   obtain a corrected elevation for each repeat that contains no selected pairs, we identify the
581   segment from that repeat that has the smallest error estimate, and report the value z_c as that
582   repeat's *ptx/h_corr*, and use $\boldsymbol{\sigma}_{z,c}$ as its error (*/ptx/h_corr_sigma*).

583   **3.5   Calculating systematic error estimates**

584   The errors that have been calculated up to this point are due to errors in fitting segments to
585   photon-counting data and due to inaccuracies in the polynomial fitting model. Additional error
586   components can result from more systematic errors, such as errors in the position of ICESat-2 as
587   derived from POD, and pointing errors from PPD. These are estimated in the ATL06
588   *sigma_geo_xt, sigma_geo_at*, and *sigma_geo_r* parameters, and their average for each repeat is
589   reported in the *cycle_stats* group under the same parameter names. The geolocation component
590   of the total height is the product of the geolocation error and the surface slope, added in
591   quadrature with the vertical height error:

12

$$\sigma_{h,systematic} = \left[\left(\frac{dh}{dx}\sigma_{geo,AT}\right)^2 + \left(\frac{dh}{dy}\sigma_{geo,XT}\right)^2 + \sigma_{geo,r}^2\right]^{1/2}$$

592   For selected segments, which generally come from pairs containing two high-quality height
593   estimates, *dh/dy* is estimated from the ATL06 *dh_fit_dy* parameter. For unselected segments, it is
594   based on the *y* component of the reference-surface slope, as calculated in section 4.2.
595   The error for a single segment's corrected height is:

$$\sigma_{h,total} = \left[\sigma_{h,systematic}^2 + \sigma_{h,c}^2\right]^{1/2}$$

13

596   This represents the total error in the surface height for a single corrected height. In most cases,
597   error estimates for averages of ice-sheet quantities will depend on errors from many segments
598   from different reference points, and the spatial scale of the different error components will need
599   to be taken into account in error propagation models. To allow users to separate these effects,
600   we report both the uncorrelated error, */ptx/h_corr_sigma,* and the component due only to
601   systematic errors, */ptx/h_corr_sigma_systematic.* The total error is the quadratic sum of the two,
602   as described in equation 13.

603   **3.6   Calculating shape-corrected heights for crossing-track data**

604   Locations where groundtracks cross provide opportunities to check the accuracy of
605   measurements by comparing surface-height estimates between the groundtracks, and also offers
606   the opportunity to generate elevation-change time series that have more temporal detail than the
607   91-day repeat cycle can offer for repeat-track measurements.
608   At these crossover points, we use the reference surface calculated in 3.5 to calculate corrected
609   elevations for the crossing tracks. We refer to the track for which we have calculated the
610   reference surface as the *datum* track, and the other track as the *crossing* track. To calculate
611   corrected surface heights for the crossing ICESat-2 orbits, we first select all data from the
612   crossing orbit within a distance *L_search_XT* of the updated reference point on the datum track.
613   For most datum reference points, this will yield no crossing data, in which case the calculation
614   for that datum point terminates. If crossing data are found, we then calculate the coordinates of
615   these points in the reference point's along-track and across-track coordinates. This calculation
616   begins by transforming the crossing-track data into local northing and easting coordinates
617   relative to the datum reference-point location:

$$\delta N_c = \frac{\pi R_e}{180}(lat_c - lat_d)$$

14

$$\delta E_c = \frac{\pi R_e}{180}(lon_c - lon_d)\cos(lat_c)$$

618   Here (lat_d, lon_d) are the coordinates of the adjusted datum reference point, (lat_c, lon_c) are the
619   coordinates of the points on the crossing track, and R_e is the local radius of the WGS84 ellipsoid.
620   We then convert the northing and easting coordinates into along-track and across-track
621   coordinates based on the azimuth ϕ of the datum track:

$$x_c = \delta N_c \cos(\phi) + \delta E_c \sin(\phi)$$

15

$$y_c = \delta N_c \sin(\phi) - \delta E_c \cos(\phi)$$

622   Using these coordinates, we proceed as we did in 3.4 and 3.5: we generate $\mathbf{S}_k$ and $\mathbf{S}_{kt}$ matrices,
623   use them to correct the data and to identify the data point with the smallest error for each

624   crossing cycle. We report the time, error estimate, and corrected height for the minimum-error
625   datapoint from each cycle, as well as the location, pair, and track number corresponding to the
626   datum point in the */ptx/crossing_track_data* group. Because the crossing angles between the
627   tracks are oblique at high latitudes, a particular crossing track may appear in a few subsequent
628   datum points; in these cases, we expect that the error estimates should vary with the distance
629   between the crossing track and the datum track, so that the point with the minimum error should
630   correspond to the precise crossing location of the two tracks.
631   To help evaluate the quality of crossing-track data we calculate the *along_track_rss* parameter
632   for each crossing-track measurement. This parameter gives the RSS of the differences between
633   each segment's endpoint heights and the heights of the previous and subsequent segments. A
634   segment that is consistent with the previous and next segments in slope and elevation will have a
635   small value for this parameter, a segment that is inconsistent (and thus potentially in error) will
636   have a large value. Crossing-track measurements that have values greater than 10 m are
637   excluded form ATL11 and do not appear in the dataset.

3.7   Calculating parameter averages

639   ATL11 contains a variety of parameters that mirror parameters in ATL06, but are averaged to the
640   140-m ATL11 resolution. Except where noted otherwise, these quantities are weighted averages
641   of the corresponding ATL06 values. For selected pairs (i.e. those included in the reference-
642   surface fit), the parameters are averaged over the selected segments from each cycle, using
643   weights derived from their formal errors, *h_li_sigma*. The parameter weighted average for the N_k
644   segments from cycle k is then:

$$\langle q \rangle = \frac{\sum_{i=1}^{N_k} |\sigma_i^{-2}| q_i}{\sum_{i=1}^{N_k} |\sigma_i^{-2}|} \qquad\qquad 16$$

645   Here q_i are the parameter values for the segments. For repeats with no selected pairs, recall that
646   the corrected height for only one segment is reported in */ptx/h_corr*; for these, we simply report
647   the corresponding parameter values for that selected segment.
648

3.8   Output data editing

650   The output data product includes cycle height estimates only for those cycles that have
651   non-systematic error estimates (*/ptx/h_corr_sigma*) less than 15 m. All other heights (and their
652   errors) are reported as *invalid*.
653

654

655 **4.0   LAND ICE PRODUCTS: LAND ICE H (T)(ATL 11/L3B)**

656   Each ATL11 file contains data for a single reference ground track, for one of the subregions
657   defined for ATLAS granules (see Figure 6-3). The ATL11 consists of three top-level groups, one
658   for each beam pair (*pt1, pt2, pt3*). Within each pair-track group, there are datasets that give the
659   corrected heights for each cycle, their errors, and the reference-point locations. Subgroups
660   (*cycle_stats,* and *ref_surf)* provide a set of data-quality parameters, and ancillary data describing
661   the fitting process, and use the same ordering and coordinates as the top-level group (i.e. any
662   dataset within the */ptx/cycle_stats* and */ptx/ref_surf* groups refers to the same latitude, longitude,
663   and reference points as the corresponding measurements in the */ptx/* groups.)   The
664   *crossing_track_data* group gives height measurements at crossover locations, and has its own set
665   of locations and
666

667   **4.1   File naming convention**

668   ATL11 files are named in the following format:
669   ATL11_*ttttgg_cccc_rrr_vv*.h5
670   Here *tttt* is the rgt number, *gg* is the granule-region number, *cccc* gives the first and last cycles of
671   along-track data included in the file (e.g. _0308_ would indicate that cycles three through eight,
672   inclusive, might be included in the along-track solution), and *rrr* is the release number. and *vv* is
673   the version number, which is set to one the first time a granule is generated for a given data
674   release, and is incremented by one if the granule is regenerated.
675

676   **4.2   */ptx* group**

677

678   Table 4-1 shows the datasets in the *ptx* groups. This group gives the principal output parameters
679   of the ATL11. The corrected repeat measurements are in */ptx/h_corr*, which gives improved
680   height measurements based on a surface fit to valid data at paired segments. The associated
681   reference coordinates, */ptx/latitude* and */ptx/longitude* give the reference point location, with
682   averaged times per repeat, */ptx/delta_time*. For repeats with no selected pairs, the corrected
683   height is that from the selected segment with the lowest error. Two error metrics are given in
684   */ptx/h_corr_sigma* and */ptx/h_corr_sigma_systematic*. The first gives the error component due to
685   ATL06 range errors and due to uncertainty in the reference surface. The second gives the
686   component due to geolocation and radial-orbit errors that are correlated at scales larger than one
687   reference point; adding these values in quadrature gives the total per-cycle error. Values are only
688   reported for */ptx/h_corr, /ptx/h_corr_sigma,* and */ptx/h_corr_sigma_systematic* for those cycles
689   whose uncorrelated errors are less than 15 m; all others are reported as *invalid.* A
690   */ptx/quality_summary* is included for each cycle, based on fit statistics from ATL06.

19

691

692   **Table 4-1 Parameters in the */ptx/* group**

Parameter	Units	Dimensions	Description
cycle_number	counts	$1 x N_{cycles}$	Cycle number for each column of the data
latitude	degrees North	$N_{pts} \times 1$	Reference point latitude
longitude	degrees East	$N_{pts} \times 1$	Reference point longitude
ref_pt	counts	$N_{pts} \times 1$	The reference point number, *m*, counted from the equator crossing of the RGT.
delta_time	seconds	$N_{pts} \times N_{cycles}$	mean GPS time for the segments for each cycle
h_corr	meters	$N_{pts} \times N_{cycles}$	the mean corrected height
h_corr_sigma	meters	$N_{pts} \times N_{cycles}$	the formal error in the corrected height
h_corr_sigma_systematic	meters	$N_{pts} \times N_{cycles}$	the magnitude of the RSS of all errors that might be correlated at scales larger than a single reference point (e.g. pointing errors, GPS errors, etc)
quality_summary	counts	$N_{pts} \times N_{cycles}$	summary flag: zero indicates high-quality cycles: where min(signal_selection_source)<=1 and min(SNR_significance) < 0.02, and ATL06_summary_zero_count >0.

693

694   **4.3   */ptx/ref_surf* group**

695   Table 4-2 describes the */ptx/ref_surf* group. This group includes parameters describing the
696   reference surface fit at each reference point. The polynomial coefficients are given in

697 */ptx/poly_ref_surf*, sorted first by total degree, then by x-component degree. Because the
698 polynomial degree is chosen separately for each reference point, enough columns are provided in
699 the */ptx/poly_ref_surf* and */ptx/poly_ref_surf_sigma* to accommodate all possible components up
700 to 2rd degree in *y* and 3th degree in *x*, and absent values are filled in with zeros. The
701 correspondence between the columns of the polynomial fields and the exponents of the *x* and *y*
702 terms are given in the */ptx/poly_exponent_x* and */ptx/poly_exponent_y* fields. The time origin for
703 the slope change is given in the group attribute */ptx/slope_change_t0*.

Table 4-2 Parameters in the */ptx/ref_surf* group

Parameter	Units	Dimensions	Description
dem_h	Meters	$N_{pts} \times 1$	DEM elevation, derived from the ATL06 *dem_h* parameter
geoid_h	Meters	$N_{pts} \times 1$	geoid elevation, derived from the ATL06 *geoid_h* parameter
complex_surface_flag	counts	$N_{pts} \times 1$	0 indicates that normal fitting was attempted, 1 indicates that the signal selection algorithm rejected too many repeats, and only a linear fit was attempted
rms_slope_fit	counts	$N_{pts} \times 1$	the RMS of the slope of the fit polynomial within 50 m of the reference point
e_slope	counts	$N_{pts} \times 1$	the mean East-component slope for the reference surface within 50 m of the reference point
n_slope	counts	$N_{pts} \times 1$	the mean North-component slope for the reference surface within 50 m of the reference point
at_slope	Counts	$N_{pts} \times 1$	Mean along-track component of the slope of the reference surface within 50 m of the reference point
xt_slope		$N_{pts} \times 1$	Mean across-track component of the slope of the reference surface within 50 m of the reference point
deg_x	counts	$N_{pts} \times 1$	Maximum degree of non-zero polynomial components in x
deg_y	counts	$N_{pts} \times 1$	Maximum degree of non-zero polynomial components in y
poly_exponent_x	counts	*1x8*	Exponents for the x factors in the surface polynomial
poly_exponent_y	counts	*1x8*	Exponents for the y factors in the surface polynomial
poly_coeffs	counts	$N_{pts} \times 8$	polynomial coefficients (up to degree 3), for polynomial components scaled by 100 m

21

poly_ref_coeffs_sigma	counts	$N_{pts} \times 8$	formal errors for the polynomial coefficients
ref_pt_number	counts	$N_{pts} \times 1$	Ref point number, counted from the equator crossing along the RGT.
x_atc	meters	$N_{pts} \times 1$	Along-track coordinate of the reference point, measured along the RGT from its first equator crossing.
y_atc	meters	$N_{pts} \times 1$	Across-track coordinate of the reference point, measured along the RGT from its first equator crossing.
rgt_azimuth	degrees	$N_{pts} \times 1$	Reference track azimuth, in degrees east of local north
slope_change_rate_x	years^{-1}	$N_{pts} \times 1$	rate of change of the x component of the surface slope
slope_change_rate_y	years^{-1}	$N_{pts} \times 1$	rate of change of the y component of the surface slope
slope_change_rate_x_sigma	years^{-1}	$N_{pts} \times 1$	Formal error in the rate of change of the x component of the surface slope
slope_change_rate_y_sigma	years^{-1}	$N_{pts} \times 1$	Formal error in the rate of change of the y component of the surface slope
misfit_chi2r	meters	$N_{pts} \times 1$	misfit chi square, divided by the number of degrees in the solution
misfit_rms	meters	$N_{pts} \times 1$	RMS misfit for the surface-polynomial fit
fit_quality	counts	$N_{pts} \times 1$	Indicates quality of the fit: 0: no problem identified 1: One or more polynomial coefficient errors larger than 10 2: One or more components of the surface slope has magnitude larger than 0.2 3: Conditions 1 and 2 both true.

704
705
706 The slope of the fit surface is given in the *ref_surf/n_slope* and *ref_surf/e_slope* parameters in
707 the local north and east directions; the corresponding slopes in the along-track and across-track
708 directions are given in the *ref_surf/xt_slope* and *ref_surf/yt_slope* parameters. For the along-
709 track points, the surface slope is calculated by evaluating the correction-surface polynomial for a
710 10-m spaced grid of points extending ±50 m in x and y around the reference point, and
711 calculating the mean slopes of these points. The calculation is performed in along-track
712 coordinates and then projected onto the local north and east vectors. The *rms_slope_fit* is
713 derived from the same set of points, and is calculated as the RMS of the standard deviations of
714 the slopes calculated from adjacent grid points, in *x* and *y*.

715

4.4   /ptx/cycle_stats group

717 The */ptx/cycle_stats* group gives summary information about the segments present for each
718 reference point. Most parameters are averaged according to equation 14, but for others (e.g.
719 */ptx/signal_selection_flag_best*, which is the minimum of the signal selection flags for the cycle)
720 **Table 4-3** describes how the summary statistics are derived.

721

722 **Table 4-3 Parameters in the */ptx/cycle_stats* group**

Parameter	Units	Dimensions	Description
ATL06_summary_zero_count	counts	$N_{pts} \times N_{cycles}$	Number of segments with *atl06_quality_summary*=0 (0 indicates the best-quality data)
h_rms_misfit	meters	$N_{pts} \times N_{cycles}$	Weighted-average RMS misfit between PE heights and along-track land-ice segment fit
r_eff	counts	$N_{pts} \times N_{cycles}$	Weighted-average effective, uncorrected reflectance for each cycle.
tide_ocean	meters	$N_{pts} \times N_{cycles}$	Weighted-average ocean tide for each cycle
dac	meters	$N_{pts} \times N_{cycles}$	Dynamic atmosphere correction (mainly the effect of atmospheric pressure on floating-ice elevation).
cloud_flg_atm	counts	$N_{pts} \times N_{cycles}$	Minimum cloud flag from ATL06: Flag indicates confidence that clouds with OT* > 0.2 are present in the lower 3 km of the atmosphere based on ATL09
cloud_flg_asr	counts	$N_{pts} \times N_{cycles}$	Minimum apparent-surface-reflectance - based cloud flag from ATL06: Flag indicates confidence that clouds with OT > 0.2 are present in the lower 3 km of the atmosphere based on ATL09
bsnow_h	meters	$N_{pts} \times N_{cycles}$	Weighted-average blowing snow layer height for each cycle
bsnow_conf	counts	$N_{pts} \times N_{cycles}$	Maximum bsnow_conf flag from ATL06: indicates the greatest (among

23

Parameter	Units	Dimensions	Description
			segments) confidence flag for presence of blowing snow for each cycle
x_atc	meters	$N_{pts} \times N_{cycles}$	weighted average of pair-center RGT y coordinates for each cycle
y_atc	meters	$N_{pts} \times N_{cycles}$	weighted mean of pair-center RGT y coordinates for each cycle
ref_pt		$N_{pts} \times N_{cycles}$	Ref point number, counted from the equator crossing along the RGT.
seg_count	counts	$N_{pts} \times N_{cycles}$	Number of segments marked as valid for each cycle. Equal to 0 for those cycles not included in the reference-surface shape fit.
min_signal_selection_source	counts	$N_{pts} \times N_{cycles}$	Minimum of the ATL06 signal_selection_source value (indicates the highest-quality segment in the cycle)
min_snr_significance	counts	$N_{pts} \times N_{cycles}$	Minimum of SNR_significance (indicates the quality of the best segment in the cycle)
sigma_geo_h	meters	$N_{pts} \times N_{cycles}$	Root-mean-weighted-square-average total vertical geolocation error due to PPD and POD
sigma_geo_at	meters	$N_{pts} \times N_{cycles}$	Root-mean-weighted-square-average local-coordinate x horizontal geolocation error for each cycle due to PPD and POD
sigma_geo_xt	meters	$N_{pts} \times N_{cycles}$	Root-mean-weighted-square-average local-coordinate y horizontal geolocation error for each cycle due to PPD and POD
h_mean	meters	$N_{pts} \times N_{cycles}$	Weighted-average of surface heights, not including the correction for the reference surface

723 *OT (optical thickness) is a measure of signal attenuation used in atmospheric calculations. This
724 parameter discussed in ICESat-2 atmospheric products (ATL09)
725

726 **4.5**   */ptx/crossing_track_data* **group**

727 The */ptx/crossing_track_data* group (Table 4-4) contains elevation data at crossover locations.
728 These are locations where two ICESat-2 pair tracks cross, so data are available from both the
729 datum track, for which the granule was generated, and from the crossing track. The data in this
730 group represent the elevations and times from the crossing tracks, corrected using the reference
731 surface from the datum track. Each set of values gives the data from a single segment on the
732 crossing track, that was selected as having the minimum error among all segments on the
733 crossing track within the 2 *L_search_XT* –by-2 *L_search_AT* window around the reference point
734 on the datum track. The systematic errors are evaluated based on the magnitude of the reference-
735 surface slope and the magnitude of the horizontal geolocation error of the crossing-track data.
736 Attributes for the group specify the track number and pair-track number of the crossing track.
737

Table 4-4 Parameters in the */ptx/crossing_track_data* group

Parameter	Units	Dimensions	Description
ref_pt	counts	$N_{XO} \times 1$	the reference-point number for the datum track
delta_time	years	$N_{XO} \times 1$	time relative to the ICESat-2 reference epoch
h_corr	meters	$N_{XO} \times 1$	WGS-84 height, corrected for the ATL11 surface shape
h_corr_sigma	meters	$N_{XO} \times 1$	error in the height estimate
h_corr_sigma_systematic	meters	$N_{XO} \times 1$	systematic error in the height estimate
ocean_tide	Meters	$N_{XO} \times 1$	Ocean-tide estimate for the crossing track
dac	Meters	$N_{XO} \times 1$	Dynamic atmosphere correction for the crossing track
latitude	degrees	$N_{XO} \times 1$	latitude of the crossover point
longitude	degrees	$N_{XO} \times 1$	longitude of the crossover point
cycle_number	counts	$N_{XO} \times 1$	Cycle number for the crossing data
rgt	counts	$N_{XO} \times 1$	The RGT number for the crossing data
spot_crossing	counts	$N_{XO} \times 1$	The spot number for the crossing data

atl06_quality_summary	counts	$N_{XO} \times 1$	quality flag for the crossing data derived from ATL06. 0 indicates no problems detected, 1 indicates potential problems
along_track_rss	meters	$N_{XO} \times 1$	Root sum of the squared differences between the heights of the endpoints for the crossing-track segment and the centers of the previous and next segments

738
739

26

740 **5.0   ALGORITHM IMPLEMENTATION**

741

742   **Figure 5-1 Flow Chart for ATL11 Surface-shape Corrections**
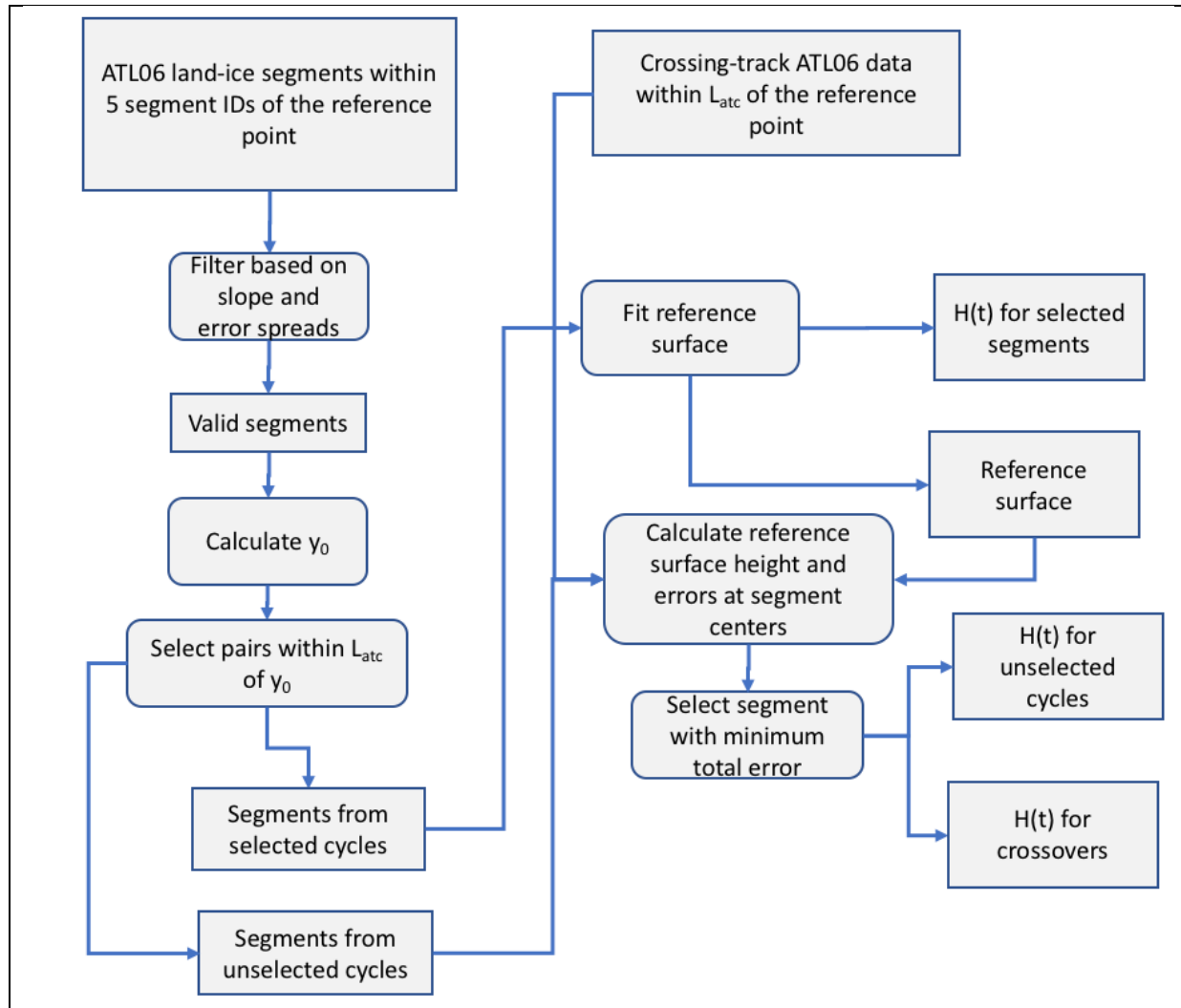
743
744
745   The following steps are performed for each along-track reference point.
746   1. Segments with *segment_id* within *N_search/2* of the reference-point number, are
747   selected.
748   2. Valid segments are identified based on estimated errors, the *ATL06_quality_summary*
749   parameter, and the along- and across-track segment slopes. Valid pairs, containing valid
750   measurements from two different beams, are also identified.
751   3. The location of the reference point is adjusted to allow the maximum number of repeats
752   with at least one valid pair to fall within the across-track search distance of the reference
753   point.

27

754   4. The reference surface is fit to pairs with two valid measurements within the search
755   distance of the reference point. This calculation also produces corrected heights for the
756   selected pairs and the errors in the correction polynomial coefficients.
757   5. The correction surface is used to derive corrected heights for segments not selected in
758   steps 1-3, and the height for the segment with the smallest error is selected for each
759   6. The reference surface is used to calculate heights for external (pre-ICESat-2) laser
760   altimetry data sets and crossover ICESat-2 data.
761 A schematic of this calculation is shown in Figure 5-1.

762 ### 5.1.1 Select ATL06 data for the current reference point

763 **Inputs:**
764 *ref_pt:* segment number for the current refererence point
765 *track_num:* The track number for current point
766 *pair_num:* The pair number for the current point
767 **Outputs:**
768 *D_ATL06:* ATL06 data structure
769 **Parameters:**
770 *N_search*: number of segments to search, around ref_pt, equal to 5.
771 **Algorithm:**
772 *1.* For each along-track point, load all ATL06 data from track *track_num* and pair *pair_num* that
773 have *segment_id* within *N_search* of *ref_pt:* These segments have *ref_pt - N_search*
774 *<=segment_id <= ref_pt +N_search.*
775 *2.* Reject any data that have *y_atc* values more than 500 m distant from the nominal pair-track
776 centers (3200 m for pair 1, 0 m for pair 2, -3200 m for pair 3).
777

778 ### 5.1.2 Select pairs for the reference-surface calculation

779 **Inputs:**
780 *ref_pt:* reference point number for the current fit
781 *x_atc_ctr*: Along-track coordinate of the reference point
782 *D_ATL06*: ATL06 data structure
783 *pair_data*: Structure describing ATL06 pairs, includes mean of strong/weak beam *y_atc* and
784 *dh_fit_dy*
785 **Outputs:**
786 *validity flags for each segment:*
787   *valid_segs.x_slope:* Segments identified as valid based on x-slope consistency
788   *valid_segs.data:* Segments identified as valid based on ATL06 parameter values.
789 *Validity flags for each pair*:
790   *valid_pairs:* Pairs selected for the reference-surface calculation
791   *valid_pairs.y_slope:* Pairs identified as valid based on y-slope consistency
792 *y_polyfit_ctr*: y center of the slope regression
793 *ref_surf/complex_surface_flag*: Flag indicating 0: non-complex surface, 1: complex surface.
794

Parameters:

795

796 *L_search_XT*: The across-track search distance.

797 *N_search*: Along-track segment search distance

798 *seg_sigma_threshold_min*: Minimum threshold for accepting errors in segment heights, equal to

799 0.05 m.

800 **Algorithm:**

801 1. Flag valid segments based on ATL06 values.

802   1a. Count the cycles that contain at least one pair that has *atl06_quality_flag*=0

803 for both segments. If this number is greater than *N_cycles/3*, set

804 *ref_surf/complex_surface_flag*=0 and set *valid_segs.data* to 1 for segments with

805 *ATL06_quality_summary* equal to 0. Otherwise, set *ref_surf/complex_surface_flag*=1 and set

806 *valid_segs.data* to 1 for segments with *snr_significance < 0.02*.

807   1b. Define *seg_sigma_threshold* as the maximum of 0.05 or three times the median of

808 *sigma_h_li* for segments with *valid_segs.data* equal to 1. Set *valid_segs.data* to 1 for segments

809 with *h_sigma_li* less than this threshold and *ATL06_quality_summary* equal to 0.

810   1c. Define *valid_pairs.data:* For each pair of segments, set *valid_pairs.data* to 1 when

811 both segments are marked as valid in *valid_segs.data*.

812 2. Calculate representative values for the *x* and *y* coordinate for each pair, and filter by distance.

813   2a. For each pair containing two defined values, set *pair_data.x* to the segments' *x_atc*

814 value, and *pair_data.y* to the mean of the segments' *y_atc* values.

815   2b. Calculate *y_polyfit_ctr*, equal to the median of *pair_data.y* for pairs marked valid in

816 *valid_pairs.data.*

817   2c. Set *valid_pairs.ysearch* to 1 for pairs with |*pair_data.y - y_polyfit_ctr*| <

818 *L_search_XT*.

819 3. Select pairs based on across-track slope consistency

820   3a. Define *pairs_valid_for_y_fit*, for the across-track slope regression if they are marked

821 as valid in *valid_pairs.data,* and *valid_pairs.ysearch,* not otherwise.

822   3b. Choose the degree of the regression for across-track slope

823   -If the valid pairs contain at least two different *x_atc* values (separated by at least

824 18 m), set the along-track degree, *my_regression_y_degree,* to 1, 0 otherwise.

825   -If valid pairs contain at least two different *ref_surf/y_atc* values (separated by at

826 least 18 m), set the across-track degree, *my_regression_y_degree,* to 1, 0 otherwise.

827   3c. Calculate the formal error in the y slope estimates: *y_slope_sigma* is the RSS of the

828 *h_li_sigma* values for the two beams in the pair divided by the difference in their *y_atc*

829 values. Based on these, calculate *my_regression_tol*, equal to the maximum of 0.01 or three

830 times the median of *y_slope_sigma* for valid pairs (*pairs_valid_for_y_fit).*

831   3d. Calculate the regression of *dh_fit_dy* against *pair_data.x* and *pair_data.y* for valid

832 pairs (*pairs_valid_for_y_fit).* The result is *y_slope_model*, which gives the variation of *dh_fit_dy*

833 as a function of *x_atc* and *y_atc.* Calculate *y_slope_resid,* the residuals between the *dh_fit_dy*

834 values and *y_slope_model* for all pairs in *pair_data*.

835   3e. Calculate *y_slope_threshold*, equal to the maximum of *my_regresion_tol* and three

836 times the RDE of *y_slope_resid* for valid pairs.

837   3f. Mark all pairs with |*y_slope_resid*| > y*_slope_threshold* as invalid. Re-establish
838 *pairs_valid_for_y_fit (*based on *valid_pairs.data, valid_pairs.y_slope* and *valid_pairs.ysearch)*.
839 Return to step 3d (allow two iterations total).

840   3g. After the second repetition of 3d-f, use the model to mark all pairs with
841 |*y_slope_resid*| less than y*_slope_threshold* with 1 in *valid_pairs.y_slope*, 0 otherwise.
842 4. Select segments based on along-track slope consistency for both segments in the pair
843   4a. Define *pairs_valid_for_x_fit*, valid segments for the along-track slope regression*:*
844 segments are valid if they come from pairs marked as valid in *valid_pairs.data* and
845 *valid_pairs.ysearch,* not otherwise.
846   4b. Choose the degree of the regression for along-track slope
847   -If valid segments contain at least two different *x_atc* values set the along-track
848 degree, *mx_regression_x_degree,* to 1, 0 otherwise.
849   -If valid segments contain at least two different *y_atc* values, set the across-track
850 degree, *mx_regression_y_degree,* to 1, 0 otherwise.
851   4c. Calculate along-track slope regression tolerance, *mx_regression_tol*, equal to the
852 maximum of either 0.01 or three times the median of the *dh_fit_dx_sigma* values for the valid
853 pairs.
854   4d. Calculate the regression of *dh_fit_dx* against *pair_data.x* and *pair_data.y* for valid
855 segments (*pairs_valid_for_x_fit*). The result is *x_slope_model*, which gives the variation of
856 *dh_fit_dx* as a function of *pair_data.x* and *pair_data.y*. Calculate *x_slope_resid*, the residuals
857 between the *dh_fit_dx* and *x_slope_resid* for all segments for this reference point, *seg_x_center*
858 and *y_polyfit_ctr*.
859   4e. Calculate *x_slope_threshold*, equal to the maximum of either *mx_regression_tol* or
860 three times the RDE of *x_slope_resid* for valid segments.
861   4f. Mark *valid_segs.x_slope* with |*x_slope_resid*| > *x_slope_threshold* as invalid. Re-
862 establish *valid_pairs.x_slope* when both *valid_segs.x_slope* equal 1. Re-establish
863 *pairs_valid_for_x_fit*. Return to step 4d (allow two iterations total).
864   4g. After the second repetition of 4d-f, mark all segments with |*x_slope_resid*| less than
865 x*_slope_threshold* with 1 in *seg_valid_xslope*, 0 otherwise. Define *valid_pairs.x_slope* as 1 for
866 pairs that contain two segments with *valid_segs.x_slope=1*, 0 otherwise.
867   5. Re-establish *valid_pairs.all.* Set equal to 1 if *valid_pairs.x_slope, valid_pairs.y_slope,*
868 and *valid_pairs.data* are all valid.
869   5a. Identify *unselected_cycle_segs*, as those *D6.cycles* where *valid_pairs.all* are False.
870

5.1.3 Adjust the reference-point y locaction to include the maximum number of cycles

873 **Inputs:**
874 *D_ATL06*: ATL06 structure for the current reference point.
875 *valid_pairs:* Pairs selected based on parameter values and along- and across-track slopes.
876 **Outputs:**
877 *ref_surf/y_atc*: Adjusted fit-point center *y.*

878 *valid_pairs*: validity masks for pairs, updated to include those identified as valid based on the
879 spatial search around *y_atc_ctr*.
880 **Parameters**:
881 *L_search_XT*: Across-track search length (equal to 110 m)
882 **Algorithm:**
883   1. Define *y0* as the median of the unique integer values of the pair center y_atc for all
884 valid pairs. Set a range of y values, *y0_shifts*, as round(*y0)* +/- 100 meters in 2-meter increments.
885   2. For each value of *y0_shifts* (*y0_shift*), set a counter, *selected_seg_cycle_count,* to the
886 number of distinct cycles for which both segments of the pair are contained entirely within the *y*
887 interval [*y0_shift- L_search_XT*, *y0_shift+ L_search_XT*]. Add to this, the number of distinct
888 cycles represented by unpaired segments contained within that interval, weighted by 0.01. The
889 sum is called *score*.
890   3. Search for an optimal y-center value (with the most distinct cycles). Set *y_best* to the
891 value of *y0_shift* that maximizes *score*. If there are multiple *y0_shift* values with the same,
892 maximum *score*, set to the median of the *y0_shift* values with the maximum *score*.
893   4. Update *valid_pairs* to include all pairs with *y_atc* within +/- L_search_XT from
894 *y_atc_ctr*.

895 **5.1.4 Calculate the reference surface and corrected heights for selected pairs**

896 **Inputs:**
897 *D_ATL06*: ATL06 structure for the current reference point, containing parameters for each
898 segment:
899   *x_atc:* along-track coordinate
900   *y_atc*: across-track coordinate
901   *delta_t:* time for the segment
902 *pair_data*: Structure containing information about ATL06 pairs. Must include:
903   *y_atc:* Pair-center across-track coordinates
904 *valid_pairs:* Pairs selected based on parameter values and along- and across-track slope.
905 *x_atc_ctr*: The reference point along-track x coordinate (equal to *ref_surf/x_atc*).
906 *y_atc_ctr*: The reference point along-track x coordinate (equal to *ref_surf/y_atc*)
907 **Outputs:**
908 *ref_surf/deg_x:* Degree of the reference-surface polynomial in the along-track direction
909 *ref_surf/deg_y:* Degree of the reference-surface polynomial in the across-track direction
910 *ref_surf/poly_coeffs*: Polynomial coefficients of the reference-surface fit
911 *ref_surf/poly_coeffs_sigma*: Formal error in polynomial coefficients of the reference-surface fit
912 *ref_surf/slope_change_rate_x*: Rate of change of the x component of the surface slope
913 *ref_surf/slope_change_rate_x_sigma*: Formal error in the rate of change of the x component of
914 the surface slope
915 *ref_surf/slope_change_rate_y*: Rate of change of the y component of the surface slope
916 *ref_surf/slope_change_rate_y_sigma*: Formal error in the rate of change of the y component of
917 the surface slope
918 *r_seg:* Segment residuals from the reference-surface model
919 */ptx/h_corr*: Partially filled-in per-cycle corrected height for cycles used in reference surface

920   */ptx/h_corr_sigma:* Partially filled-in per-cycle formal error in corrected height for cycles used in
921   reference surface
922   *ref_surf_cycles*: A list of cycles used in defining the reference surface
923   *C_m_surf*: Covariance matrix for the reference-polynomial and surface-change model
924   *fit_columns_surf:* Mask identifying which components of the combined reference-polynomial
925   and surface-change model were included in the fit.
926   *poly_exponent_x:* The x degrees corresponding to the columns of matrix used in fitting the
927   reference surface to the data
928   *poly_exponent_y:* The y degrees corresponding to the columns of matrix used in fitting the
929   reference surface to the data
930   *selected_segments:* A set of flags indicating which segments were selected by the iterative
931   fitting process.
932   Partially filled-n per-cycle ATL11 output variables (see table 4-3) for cycles used in reference
933   surface
934   **Parameters:**
935   *poly_max_degree_AT:* Maximum polynomial degree for the along-track fit, equal to 3.
936   *poly_max_degree_XT:* Maximum polynomial degree for the across-track fit, equal to 2.
937   *slope_change_t0:* Half the duration of the mission (equal to the time of the last-possible
938   elevation value minus the time of the start of data collection, divided by two).
939   *max_fit_iterations*: Maximum number of iterations for surface fitting, with acceptable residuals,
940   equal to 20.
941   *xy_scale:* The horizontal scaling value used in polynomial fits, equal to 100 m
942   *t_scale*: The time scale used in polynomial fits, equal to seconds in 1 year.
943   **Algorithm**:
944   　　　1. Build the cycle design matrix: **G_zp** is a matrix that has one column for each distinct
945   cycle in *selected_pairs* and one row for each segment whose pair is in *selected pairs*. For each
946   segment, the corresponding row of **G_zp** is 1 for the column matching the cycle for that segment
947   and zero otherwise.
948   　　　2. Select the polynomial degree.
949   　　　　The degree of the *x* polynomial, *ref_surf/deg_x,* is:
950   *min(poly_max_degree_AT,* maximum(number of distinct values of *round((x_atc- x_atc_ctr)/20)*
951   among the selected segments in any one cycle) -1), and the degree of the *y* polynomial,
952   *ref_surf/deg_y,* is : *min(poly_max_degree_XT,* number of distinct values of
953   *round((pair_data.y_atc-y_atc_ctr)/20)* among the selected pairs)
954   　　　3. Perform an iterative fit for the reference-surface polynomial.
955   　　　3a. Define *degree_list_x* and *degree_list _y*: This array defines the *x* and *y* degree of the
956   polynomial coefficients in the polynomial surface model.   There is one component for each
957   unique degree combination of *x* degrees between 0 and *ref_surf/deg_x* and for *y* degree between
958   0 and *ref_surf/deg_y* such that *x_degree + y_degree <= max(ref_surf/deg_x, ref_surf/deg_y)*,
959   except that there is no *x_degree=0* and *y_degree=0* combination. They are sorted first by the
960   sum of the *x* and *y* degrees, then by *x* degree, then by *y* degree.
961   　　　3b. Define the polynomial fit matrix. **S_fit_poly** has one column for each element of
962   the polynomial degree arrays, with values equal to $((x\_atc - x\_atc\_ctr)/xy\_scale)^{x\_degree} ((y\_atc-$
963    $y\_atc\_ctr)/xy\_scale)^{y\_degree}$. There is one row in the matrix for every segment marked as *selected*.

32

964   3c. If the time span is longer than 1.5 years, define slope-change matrices,
965   **S_fit_slope_change**. The first column of the matrix gives the rate of slope change in the x
966   component, equal to *(x_atc- x_atc_ctr)/xy_scale*(delta_time-slope_change_t0)/t_scale*. The
967   second column gives the rate of slope change in the y component, equal to *(y_atc-*
968   *y_atc_ctr)/xy_scale*(delta_time-slope_change_t0)/t_scale*.
969   3d. Build the surface matrix, **G_surf**, and the combined surface and cycle-height matrix,
970   **G_surf_zp**: The surface matrix is equal to the horizontal catenation of **S_fit_poly**, and, if
971   defined, **S_fit_slope_change.** The combined surface and cycle-height matrix, **G_surf_zp,** is
972   equal to the horizontal catenation of **G_surf** and **G_zp.**
973   3e. Subset the fitting matrix. Subset **G_surf_zp** by row to include only rows
974   corresponding to selected segments to produce **G** (on the first iteration, all are *selected*). Next,
975   subset **G** by column, first to eliminate all-zero columns, and second to include only columns that
976   are linearly independent from one another: calculate the normalized correlation between each
977   pair of columns in G, and if the correlation is equal to unity, eliminate the column with the
978   higher weighted degree (*poly_wt_sum = x_degree* + 1.1*y_degree, with the factor of 1.1
979   chosen to avoid ties). Identify the selected columns in the matrix as *fit_columns*. If more than
980   three of the original surface-change columns have been eliminated, set the
981   *ref_surf/complex_surface_flag* to *True*, mark all columns corresponding to polynomial
982   coefficients of combined x and y degree greater than 1 as *False* in *fit_columns*.
983   3f. Check whether the inverse problem is under- or even-determined: If the number of
984   *selected_segments* is less than the number of columns of **G**, eliminate remaining columns of **G** in
985   descending order of *poly_wt_sum* until the number of columns of **G** is less than the number of
986   *selected_segments.*
987   3g. Generate the data-covariance matrix, **C_d**. The data-covariance matrix is a square
988   matrix whose diagonal elements are the squares of the *h_li_sigma* values for the selected
989   segments.
990   3h. Calculate the polynomial fit. Initialize *m_surf_zp***,** the reference model, to a vector of
991   zero values, with one value for each column of **G_surf_zp**. Calculate the generalized inverse
992   (equation 7) , of **G**, **G_g.** If the inversion calculation returns an error, or if any row of **G_g** is all-
993   zero (indicating some parameters are not linearly independent), report fit failure and return.
994   Otherwise, multiply **G_g** by the subset of *h_li* corresponding to the selected segment to give *m***,**
995   containing values for the parameters selected in *fit_columns*. Fill in the components of
996   *m_surf_zp* flagged in *fit_columns* with the values in *m.*
997   3i. Calculate model residuals for all segments, *r_seg*, equal to *h_li*-**G_surf_dz** *
998   *m_surf_zp*. The subset of *r_seg* corresponding to *selected* segments is *r_fit.*
999   3j. Calculate the fitting tolerance, *r_tol*, equal to three times the RDE of the
1000   *r_fit/h_li_sigma* for all *selected* segments. Calculate the reduced chi-squared value for these
1001   residuals, *ref_surf/misfit_chi2*, equal to $r\_fit^T C\_d^{-1} r\_fit$. Calculate the *P* value for the misfit,
1002   equal to one minus the CDF of a chi-squared distribution with *m-n* degrees of freedom for
1003   *ref_surf/misfit_chi2*, where *m* is the number of rows in **G**, and *n* is the number of columns.
1004   3k. If the *P* value is less than 0.025 and fewer than *max_fit_iterations* have taken place,
1005   mark all segments for which |*r_seg/h_li_sigma*| < *r_tol* as *selected*, and return to 3e. Otherwise,
1006   continue to 3k.

1007   3l. Propagate the errors. Based on the most recent value of **C_d**, generate a revised data-
1008   covariance matrix, **C_dp**, whose diagonals values are the maximum of $h\_li\_sigma^2$ and
1009   RDE(r_fit)^2. Calculate the model covariance matrix, **C_m** using equation 9. If any of the
1010   diagonal elements of **C_m** are larger than 10^4, report a fit failure and return. Fill in elements of
1011   ***m_surf_zp*** that are marked as valid in *fit_columns* with the square roots of the corresponding
1012   diagonal elements of **C_m**. If any of the errors in the polynomial coefficients are larger than 10,
1013   set *ref_surf/fit_quality*=1.
1014   4. Return a list of cycles used in determining the reference surface in *ref_surf_cycles*. These
1015   cycles have columns in **G** that contain a valid pair, and for which the steps 3e and 3j did not
1016   eliminate the degree of freedom. For these cycles, partially fill in the values of */ptx/h_corr* and
1017   */ptx/h_corr_sigma,* from ***m*** and ***m_sigma***. Similarly, fill in values for
1018   */ptx/h_corr_sigma_systematic (*Equation 12*) and /ptx/delta_time,* as well as all variables in Table
1019   4-3. Set */ptx/h_corr, /ptx/h_corr_sigma, /ptx/h_corr_sigma_systematic* to *NaN* for those cycles
1020   that have uncorrelated error estimates greater than 15 m.
1021   Values from Table 4-2 defining the fitted reference surface are also reported including
1022   *ref_surf/poly_coeffs,* and *ref_surf/poly_coeffs_sigma*, *ref_surf/slope_change_rate_x,*
1023   *ref_surf/slope_change_rate_y, ref_surf/slope_change_rate_x_sigma,* and
1024   *ref_surf/slope_change_rate_y_sigma*.
1025   Return **C_m_surf**, the portion of **C_m** corresponding to the polynomial and slope-change
1026   components of **C_m**. Return *selected_cols_surf*, the subset of *selected_cols* corresponding to the
1027   surface polynomial and slope-change parameters.
1028   Return the reduced chi-square value for the last iteration, *ref_surf/misfit_chi2r*, equal to
1029   *ref_surf/misfit_chi2/(m-n)*.
1030

5.1.5   Calculate corrected heights for cycles with no selected pairs.

1032   **Inputs:**

1033   **C_m_surf**: Covariance matrix for the reference-surface model.
1034   *degree_list_x, degree_list_y:* List of x-, y-, degrees for which the reference-surface calculation
1035   attempted an estimate.
1036   *selected_cols_surf:* Parameters of the combined reference-surface and slope-change model for
1037   which the inversion returned a value. There should be one value for each row/column of
1038   **C_m_surf**.
1039   *x_atc_ctr, y_atc_ctr*: Center point for the surface fit (equal to *ref_surf/x_atc, ref_surf/y_atc*)
1040   *selected_segments*: Boolean array indicating segments selected for the reference-surface
1041   calculation
1042   *valid_segs.x_slope:* Segments identified as valid based on x-slope consistency
1043   *valid_segs.data:* Segments identified as valid based on ATL06 parameter values.
1044   *pair_number:* Pair number for each segment
1045   *h_li:* Land-ice height for each segment
1046   *h_li_sigma*: Formal error in *h_li.*
1047   */ptx/h_corr:* Partially filled-in per-cycle corrected height
1048   */ptx/h_corr_sigma:* Partially filled-in per-cycle corrected height error

1049   *ref_surf/poly_coeffs*: Polynomial coefficients from 2-d reference-surface fit
1050   *ref_surf_cycles*: A list of cycles used in defining the reference surface
1051   *ref_surf/slope_change_rate_x, ref_surf/slope_change_rate_y*: Rate of change of the x and y
1052   components of the surface slope
1053   *ref_surf/N_slope, ref_surf/E_slope*: slope components of reference surface
1054   *sigma_geo_r:* Radial component of the geolocation error for the crossing track
1055   *D_ATL06:* ATL06 data structure
1056   Partially filled-in per-cycle ATL11 output variables (see table 4-3)
1057   **Outputs:**
1058   */ptx/h_corr:* Per-cycle corrected height
1059   */ptx/h_corr_sigma:* Per-cycle corrected height error
1060   *selected_segments:* A set of arrays listing the selected segments for each cycle.
1061   Per-cycle ATL11 output variables (see table 4-3).
1062   **Algorithm:**
1063   1. Identify the segments marked as valid in *valid_segs.data* and *valid_segs.x_slope* that are not
1064   members of the cycles in *ref_surf_cycles*. Label these as *non_ref_segments.*
1065   2. Build **G_other**, a polynomial-fitting matrix for the *non_ref_segments.* **G_other** will include
1066   only the polynomial components listed in *degree_list_x* and *degree_list_y*, and (if the mission
1067   has been going on for at least 1.5 years) the slope-change components. Multiply **G_other** by
1068   [*ref_surf/poly_coeffs, ref_surf/slope_change_rate_x, ref_surf/slope_change_rate_y*] to give
1069   corrected heights, *z_kc*.
1070   3. Take the subset of **G_other** corresponding to the components in *fit_cols_surf* to make
1071   **G_other_surf**. Propagate the polynomial surface errors and surface-height errors for
1072   *non_ref_segments* based on **G_other_surf**, **C_m_surf,** and *h_li_sigma* using equation
1073   11. These errors are *z_kc_sigma*.
1074   4. Identify the segments in *non_ref_segments* for each cycle, and, from among these, select the
1075   one with the smallest *z_kc_sigma.* If, for this cycle, *z_kc_sigma* is less than 15 m, fill in the
1076   corresponding values of */ptx/h_corr* and */ptx/h_corr_sigma*. For cycles containing no valid
1077   segments, report invalid data as NaN. Similarly, fill in the variables in Table 4-3, with the value
1078   from the segment with the smallest *z_kc_sigma*.
1079

1080   ### 5.1.6 Calculate corrected heights for crossover data points

1081   **Inputs:**
1082   *C_m_surf*: Covariance matrix for the reference surface model.
1083   *C_m_surf*: Covariance matrix for the reference-surface model.
1084   *x_atc_ctr, y_atc_ctr*: Center point for the surface fit, in along-track coordinates
1085   *lat_d, lon_d:* Latitude and longitude for the adjusted datum reference point (from */ptx/latitude,*
1086   */ptx/longitude*)
1087   *PT:* Pair track for the surface fit
1088   *RGT:* RGT for the surface fit
1089   *ref_surf/rgt_azimuth:* The azimuth of the RGT, relative to local north
1090   *lat_c, lon_c:* Location for crossover data
1091   *time_c:* Time for crossover data

1092 *h_c:* Elevations for crossover data
1093 *sigma_h_c:* Estimated errors for crossover data
1094 **Outputs:**
1095 *ref_pt:* reference point (for the reference track)
1096 *pt*: pair track for the crossing-track points
1097 *crossing_track_data/rgt:* Reference ground track for the crossing-track point
1098 *crossing_track_data/delta_time*: time for the crossing-track point
1099 *crossing_track_data/h_corr*: corrected elevation for the crossing-track points
1100 *crossing_track_data/h_corr_sigma*: error in the corrected elevation for the crossing_track points
1101 *crossing_track_data/h_corr_sigma_systematic*: Error component in the corrected elevation due
1102 to pointing and orbital errors.
1103 *crossing_track_data/along_track_rss*:
1104 **Parameters:**
1105 *L_search_XT*: Across-track search distance
1106 **Algorithm (executed independently for the data from each cycle of the mission):**
1107 1. Project data points into the along-track coordinate system:
1108   1a: Calculate along-track and across-track vectors:
1109   x_hat=[cos(ref_surf/rgt_azimuth), sin(ref_surf/rgt_azimuth)]
1110   y_hat=[sin(ref_surf/rgt_azimuth), -cos(ref_surf/rgt_azimuth)]
1111   1b. Calculate the R_earth, the WGS84 radius at lat_d.

1112   1c: Project the crossover data points into a local projection centered on the fit
1113 center:

1114   N_d= R_earth (lat_c-lat_d)
1115   E_d= R_earth cos(lat_d) (lon_c-lon_d)
1116   1d: Calculate the x and y coordinates for the data points, relative to the fit-center point:
1117   dx_c=<x_hat, [E_c, N_c]>
1118   dy_c=<y_hat, [E_c, N_c]>
1119   Here <**a,b**> is the inner (dot) product of **a** and **b**.
1120 2. Calculate the fitting matrix using equation 6.
1121 3. Calculate the errors at each point using the fitting matrix and *C_m,* using on equation 11.
1122 4. Select the minimum-error data point and report the values in Table 4-1.
1123 5. Calculate the systematic error in the corrected height:
1124   crossing_track_data/h_sigma_sigma_systematic = (*sigma_geo_r²*+ (N_d
1125 *ref_surf/n_slope*)² + ((E_d *ref_surf/e_slope*)²)$^{1/2}$
1126 6. Calculate the along-track RSS for the selected segment. For each selected crossing segment
1127 calculate the endpoint heights (equal to the segment center height plus or minus 20 meters times
1128 the segment's along-track slope), and calculate the RSS of the differences between these heights
1129 and the center heights of the previous and subsequent segments. If this RSS difference is greater
1130 than 10 m for any cycle, do not report any parameters for that segment's cycle.

1131 **5.1.7 Provide error-averaged values for selected ATL06 parameters**

1132 **Inputs**:
1133 *ATL06 data structure:* ATL06 data to be averaged

1134 *Selected_segments:* A set of arrays listing the selected segments for each cycle.
1135 *Paramteter_list:*   A list of parameters to be averaged
1136 **Outputs:**
1137 *Parameter_averages:*   One value for each parameter and each cycle
1138 **Algorithm:**
1139 1. For each cycle, select the values of *h_li_sigma* based on the values within *selected_segments*.
1140 Calculate a set of weights, *w_i*, such that the sum of the weights is equal to 1 and each weight is
1141 proportional to the inverse square of *h_li_sigma*. If only one value is present in
1142 *selected_segments*, *w_1=1*.
1143 2. For each parameter, multiply the weights for each cycle by the parameter values, report the
1144 averaged value in *parameter_averages*.

1145 **5.1.8   Provide miscellaneous ATL06 parameters**

1146 **Inputs:**
1147 *ATL06 data structure:* ATL06 data to be averaged
1148 *Selected_segments:* A set of arrays listing the selected segments for each cycle.
1149 **Outputs:**
1150   Weighted-averaged parameter values, with one value per cycle, filled in with NaN for cycles
1151 with no selected segments
1152   *cycle_stats/h_robust_sprd*
1153   *cycle_stats/h_li_rms_mean*
1154   *cycle_stats/r_eff*
1155   *cycle_stats/tide_ocean*
1156   *cycle_stats/dac*
1157   *cycle_stats/bsnow_h*
1158   *cycle_stats/x_atc*
1159   *cycle_stats/y_atc*
1160   *cycle_stats/sigma_geo_h*
1161   *cycle_stats/sigma_geo_at*
1162   *cycle_stats/sigma_geo_xt*
1163   *cycle_stats/h_mean*
1164   *ref_surf/dem_h*
1165   *ref_surf/geoid_h*
1166 Parameter minimum values, with one value per cycle, filled in NaN for cycles with no selected
1167 segments:
1168   *cycle_stats/cloud_flg_asr*
1169   *cycle_stats/cloud_flg_atm*
1170   *cycle_stats/bsnow_conf*
1171 Other parameters:
1172   *cycle_stats/strong_spot:* The laser beam number for the strong beam in the pair
1173 **Algorithm:**
1174 1. Select the segments for the cycle indicated in *selected_segments* from the
1175 *ATL06_data_structure*.
1176 2: Based on *h_li_sigma,* calculate the segment weights using equation 14.

37

1177   3.1 For ATL06 parameters *h_robust_sprd, h_li_rms, r_eff, tide_ocean, dac, bsnow_h, x_atc,*
1178   *y_atc, sigma_geo_h, sigma_geo_at, sigma_geo_xt,* and *h_mean* calculate the weighted average
1179   of the parameter based on the segment weights. The output parameter names are the same as the
1180   input parameter names, in the cycle_stats group.
1181   3.2 For ATL06 parameters *dem_h* and *geoid_h,* by regression between the measurement
1182   location and the reference point location. The output parameter names are the same as the input
1183   parameter names, in the *ref_surf* group.
1184   4. For ATL06 parameters *cloud_flg_asr* and *cloud_flg_atm* report the best (minimum) value
1185   from among the selected values. For *bsnow_conf* report the maximum value from among the
1186   selected values.
1187   5. For the cycle_stats/*strong_spot* attribute, report the laser beam number for the strong beam in
1188   the pair.
1189

5.1.9 Characterize the reference surface

Inputs:

poly_coeffs: Coefficients of the surface polynomial

poly_coeff_sigma: Error estimates for the surface polynomial

degree_list_x, degree_list_y: exponents of the reference-surface polynomial for which the
reference-surface fit returned a coefficient

rgt_azimuth: the azimuth of the reference ground track

Parameters:

poly_max_degree_AT, poly_max_degree_XT: Maximum polynomial degree allowed in x and y.

Outputs:

ref_surf/n_slope: the north component of the reference-surface slope

ref_surf/e_slope: the east component of the reference-surface slope

ref_surf/at_slope: the along-track component of the reference-surface slope

ref_surf/xt_slope: the across-track component of the reference-surface slope

ref_surf/rms_slope_fit: the rms slope of the reference surface

ref_surf/poly_ref_surf: the polynomial reference surface coefficients

ref_surf/poly_ref_surf_sigma: error estimates for *ref_surf/poly_ref_surf*

1207 **Procedure**:

1208 1. Calculate the coordinates of a grid of northing and easting offsets around the reference points,
1209 each between -50 m and 50 m in 10-meter increments: dN, dE

1210 2. Translate the coordinates into along and across-track coordinates:

1211 *dx=cos(rgt_azimuth)*dN + sin(rgt_azimuth)*dE*

1212 *dy=sin(rgt_azimuth)*dN – cos(rgt_azimuth)*dE*

1213 3. Calculate the polynomial surface elevations for the grid points by evaluating the polynomial
1214 surface at *dx* and *dy*: *z_poly*

1215 4. Fit a plane to *z_poly* as a function of *dN* and *dE*. The North coefficient of the plane is
1216 *ref_surf/n_slope*, the east component is ref_surf/e_slope, the RMS misfit of the plane is
1217 *ref_surf/rms_slope_fit*. If either component of the slope has a magnitude larger than 0.2, add 2 to
1218 *ref_surf/fit_quality*.

1219 5. Fit a plane to *z_poly* as a function of *dx* and *dy*. The along-track coefficient of the plane is
1220 *ref_surf/at_slope*, the across-track component is *ref_surf/xt_slope*.

1221   6. Generate the polynomial exponents for the output columns. The list of components for
1222 the output variables has one component for each unique degree combination of *x* degrees
1223 between 0 and *ref_surf/deg_x* and for *y* degree between 0 and *ref_surf/deg_y* such that *x_degree*
1224 *+ y_degree <= max(poly_max_degree_XT, poly_max_degree_AT)*, except that there is no
1225 *x_degree=0* and *y_degree=0* combination. They are sorted first by the sum of the *x* and *y*
1226 degrees, then by *x* degree, then by *y* degree.
1227 Match the polynomial degrees for this reference point's coefficients to these degrees, and write
1228 each value of *poly_ref_surf* and *poly_ref_surf_sigma* into the appropriate position of the output
1229 array, filling missing values with *invalid.*

1230

1231 **6.0   APPENDIX A: GLOSSARY**

1232   This appendix defines terms that are used in ATLAS ATBDs, as derived from a document
1233   circulated to the SDT, written by Tom Neumann.   Some naming conventions are borrowed from
1234   **Spots, Channels and Redundancy Assignments** (ICESat-2-ATSYS-TN-0910) by P. Luers.
1235   Some conventions are different than those used by the ATLAS team for the purposes of making
1236   the data processing and interpretation simpler.
1237
1238   **Spots.** The ATLAS instrument creates six spots on the ground, three that are weak and three that
1239   are strong, where strong is defined as approximately four times brighter than weak. These
1240   designations apply to both the laser-illuminated spots and the instrument fields of view. The
1241   spots are numbered as shown in Figure 1. At times, the weak spots are leading (when the
1242   direction of travel is in the ATLAS +x direction) and at times the strong spots are leading.
1243   However, the spot number does not change based on the orientation of ATLAS. The spots are
1244   always numbered with 1L on the far left and 3R on the far right of the pattern. Not: beams,
1245   footprints.
1246
1247   **Laser pulse (pulse for short).** Individual pulses of light emitted from the ATLAS laser are
1248   called laser pulses. As the pulse passes through the ATLAS transmit optics, this single pulse is
1249   split into 6 individual transmit pulses by the diffractive optical element. The 6 pulses travel to
1250   the earth's surface (assuming ATLAS is pointed to the earth's surface). Some attributes of a laser
1251   pulse are the wavelength, pulse shape and duration. Not: transmit pulse, laser shot, laser fire.
1252
1253   **Laser Beam.** The sequential laser pulses emitted from the ATLAS instrument that illuminate
1254   spots on the earth's surface are called laser beams. ATLAS generates 6 laser beams. The laser
1255   beam numbering convention follows the ATLAS instrument convention with strong beams
1256   numbered 1, 3, and 5 and weak beams numbered 2, 4, and 6 as shown in the figures. Not:
1257   beamlet.
1258
1259   **Transmit Pulse.** Individual pulses of light emitted from the ICESat-2 observatory are called
1260   transmit pulses. The ATLAS instrument generates 6 transmit pulses of light from a single laser
1261   pulse. The transmit pulses generate 6 spots where the laser light illuminates the surface of the
1262   earth. Some attributes of a given transmit pulse are the wavelength, the shape, and the energy.
1263   Some attributes of the 6 transmit pulses may be different. Not: laser fire, shot, laser shot, laser
1264   pulse.
1265
1266   **Reflected Pulse.** Individual transmit pulses reflected off the surface of the earth and viewed by
1267   the ATLAS telescope are called reflected pulses. For a given transmit pulse, there may or may
1268   not be a reflected pulse. Not: received pulse, returned pulse.
1269
1270   **Photon Event.** Some of the energy in a reflected pulse passes through the ATLAS receiver
1271   optics and electronics. ATLAS detects and time tags some fraction of the photons that make up
1272   the reflected pulse, as well as background photons due to sunlight or instrument noise. Any

1273 photon that is time tagged by the ATLAS instrument is called a photon event, regardless of
1274 source. Not: received photon, detected photon.
1275
1276 **Reference Ground Track (RGT).** The reference ground track (RGT) is the track on the earth at
1277 which a specified unit vector within the observatory is pointed. Under nominal operating
1278 conditions, there will be no data collected along the RGT, as the RGT is spanned by GT2L and
1279 GT2R (which are not shown in the figures, but are similar to the GTs that are shown). During
1280 spacecraft slews or off pointing, it is possible that ground tracks may intersect the RGT. The
1281 precise unit vector has not yet been defined. The ICESat-2 mission has 1387 RGTs, numbered
1282 from 0001xx to 1387xx. The last two digits refer to the cycle number. Not: ground tracks, paths,
1283 sub-satellite track.
1284
1285 **Cycle Number.** Over 91 days, each of the 1387 RGTs will be targeted in the Polar Regions
1286 once. In subsequent 91-day periods, these RGTs will be targeted again. The cycle number
1287 tracks the number of 91-day periods that have elapsed since the ICESat-2 observatory entered the
1288 science orbit. The first 91-day cycle is numbered 01; the second 91-day cycle is 02, and so on.
1289 At the end of the first 3 years of operations, we expect the cycle number to be 12. The cycle
1290 number will be carried in the mid-latitudes, though the same RGTs will (in general) not be
1291 targeted more than once.
1292
1293 **Sub-satellite Track (SST).** The sub-satellite track (SST) is the time-ordered series of latitude
1294 and longitude points at the geodetic nadir of the ICESat-2 observatory. In order to protect the
1295 ATLAS detectors from damage due to specular returns, and the natural variation of the position
1296 of the observatory with respect to the RGT throughout the orbit, the SST is generally not the
1297 same as the RGT. Not: reference ground track, ground track.
1298
1299 **Ground Tracks (GT).** As ICESat-2 orbits the earths, sequential transmit pulses illuminate six
1300 ground tracks on the surface of the earth. The track width is approximately 10m wide. Each
1301 ground track is numbered, according to the laser spot number that generates a given ground
1302 track. Ground tracks are therefore always numbered with 1L on the far left of the spot pattern
1303 and 3R on the far right of the spot pattern. Not: tracks, paths, reference ground tracks, footpaths.
1304
1305 **Reference Pair Track (RPT).** The reference pair track is the imaginary line halfway between
1306 the planned locations of the strong and weak ground tracks that make up a pair. There are three
1307 RPTs: RPT1 is spanned by GT1L and GT1R, RPT2 is spanned by GT2L and GT2R (and may be
1308 coincident with the RGT at times), and RPT3 is spanned by GT3L and GT3R. Note that this is
1309 the planned location of the midway point between GTs. We will not know this location very
1310 precisely prior to launch. Not: tracks, paths, reference ground tracks, footpaths, pair tracks.
1311
1312 **Pair Track (PT).** The pair track is the imaginary line half way between the actual locations of
1313 the strong and weak ground tracks that make up a pair. There are three PTs: PT1 is spanned by
1314 GT1L and GT1R, PT2 is spanned by GT2L and GT2R (and may be coincident with the RGT at
1315 times), and PT3 is spanned by GT3L and GT3R. Note that this is the actual location of the

41

1316 midway point between GTs, and will be defined by the actual location of the GTs. Not: tracks,
1317 paths, reference ground tracks, footpaths, reference pair tracks.
1318
1319 **Pairs.** When considered together, individual strong and weak ground tracks form a pair.   For
1320 example, GT2L and GT2R form the central pair of the array. The pairs are numbered 1 through
1321 3: Pair 1 is comprised of GT1L and GT1R, pair 2 is comprised of GT2L and GT2R, and pair 3 is
1322 comprised of GT3L and 3R.
1323
1324 **Along-track.** The direction of travel of the ICESat-2 observatory in the orbit frame is defined as
1325 the along-track coordinate, and is denoted as the +x direction. The positive x direction is
1326 therefore along the Earth-Centered Earth-Fixed velocity vector of the observatory. Each pair has
1327 a unique coordinate system, with the +x direction aligned with the Reference Pair Tracks.
1328
1329 **Across-track.** The across-track coordinate is y and is positive to the left, with the origins at the
1330 Reference Pair Tracks.
1331
1332 **Segment.** An along-track span (or aggregation) of PE data from a single ground track or other
1333 defined track is called a segment. A segment can be measured as a time duration (e.g. from the
1334 time of the first PE to the time of the last PE), as a distance (e.g. the distance between the
1335 location of the first and last PEs), or as an accumulation of a desired number of photons.
1336 Segments can be as short or as long as desired.
1337
1338 **Signal Photon.** Any photon event that an algorithm determines to be part of the reflected pulse.
1339
1340 **Background Photon.** Any photon event that is not classified as a signal photon is classified as a
1341 background photon.   Background photons could be due to noise in the ATLAS instrument (e.g.
1342 stray light, or detector dark counts), sunlight, or mis-classified signal photons. Not: noise
1343 photon.
1344
1345 **h_**.**   Signal photons will be used by higher-level products to determine height above the
1346 WGS-84 reference ellipsoid, using a semi-major axis (equatorial radius) of 6378137m and a
1347 flattening of 1/298.257223563. This can be abbreviated as 'ellipsoidal height' or 'height above
1348 ellipsoid'. These heights are denoted by h; the subscript ** will refer to the specific algorithm
1349 used to determine that elevation (e.g. is = ice sheet algorithm, si = sea ice algorithm, etc…). Not:
1350 elevation.
1351
1352 **Photon Cloud.** The collection of all telemetered photon time tags in a given segment is the (or
1353 a) photon cloud. Not: point cloud.
1354
1355 **Background Count Rate.** The number of background photons in a given time span is the
1356 background count rate. Therefore a value of the background count rate requires a segment of PEs
1357 and an algorithm to distinguish signal and background photons. Not: Noise rate, background
1358 rate.
1359

1360   **Noise Count Rate.** The rate at which the ATLAS instrument receives photons in the absence of
1361   any light entering the ATLAS telescope or receiver optics. The noise count rate includes PEs
1362   due to detector dark counts or stray light from within the instrument. Not: noise rate,
1363   background rate, and background count rate.
1364
1365   **Telemetry band.** The subset of PEs selected by the science algorithm on board ATLAS to be
1366   telemetered to the ground is called the telemetry band. The width of the telemetry band is a
1367   function of the signal to noise ratio of the data (calculated by the science algorithm onboard
1368   ATLAS), the location on the earth (e.g. ocean, land, sea ice, etc…), and the roughness of the
1369   terrain, among other parameters. The widths of telemetry bands are adjustable on-orbit. The
1370   telemetry bandwidth is described in Section 7 or the ATLAS Flight Science Receiver Algorithms
1371   document. The total volume of telemetered photon events must meet the data volume constraint
1372   (currently 577 GBits/day).
1373
1374   **Window, Window Width, Window Duration.** A subset of the telemetry band of PEs is called a
1375   window. If the vertical extent of a window is defined in terms of distance, the window is said to
1376   have a width. If the vertical extent of a window is defined in terms of time, the window is said to
1377   have a duration. The window width is always less than or equal to the telemetry band.
1378
1379
1380
1381
1382

Figure 6-1. Spots and tracks, forward flight

Spot and track naming convention with ATLAS oriented in the forward (instrument coordinate +x) direction.

1383
1384
1385
1386
1387
1388
1389
1390
1391
1392
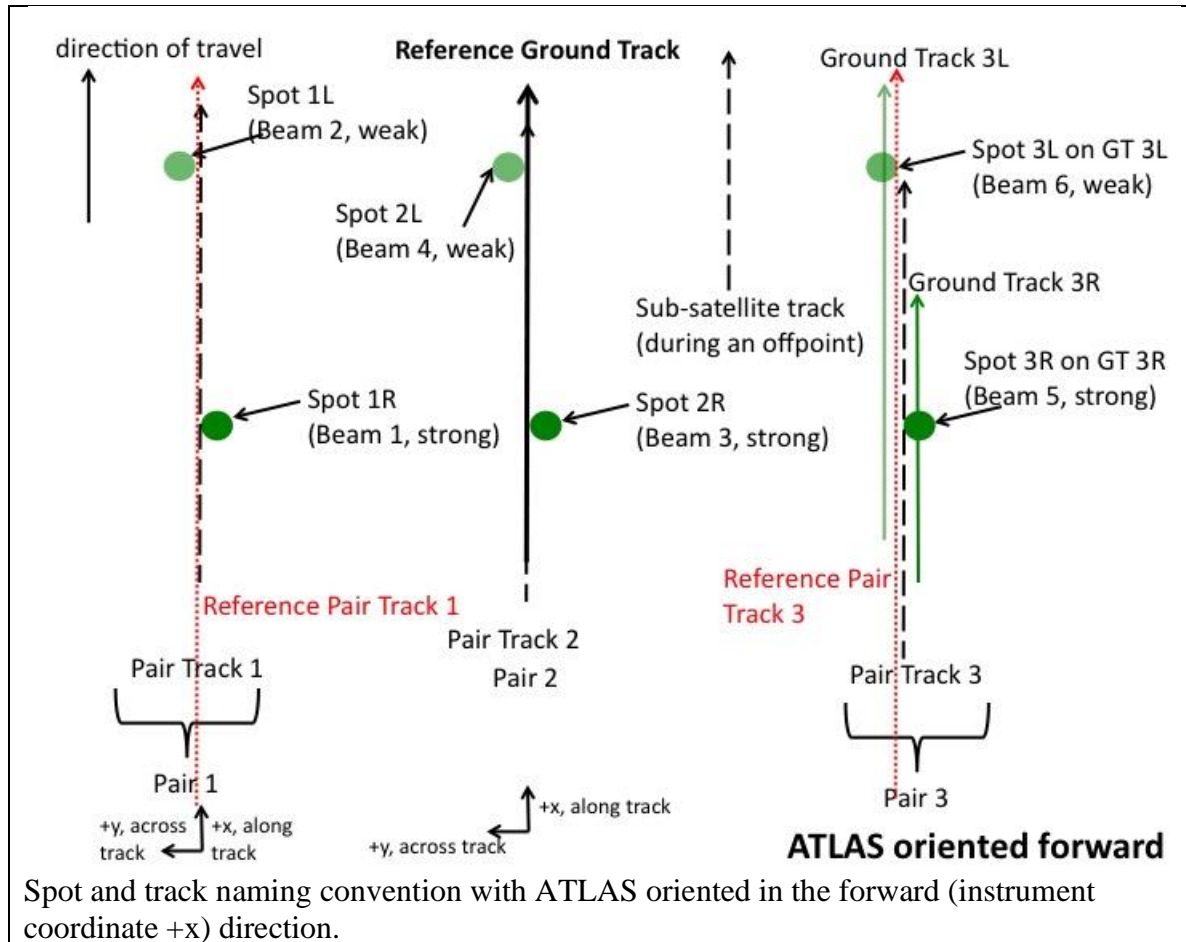
Figure 6-2. Spots and tracks, backward flight

Spot and track naming convention with ATLAS oriented in the backward (instrument coordinate -x) direction.
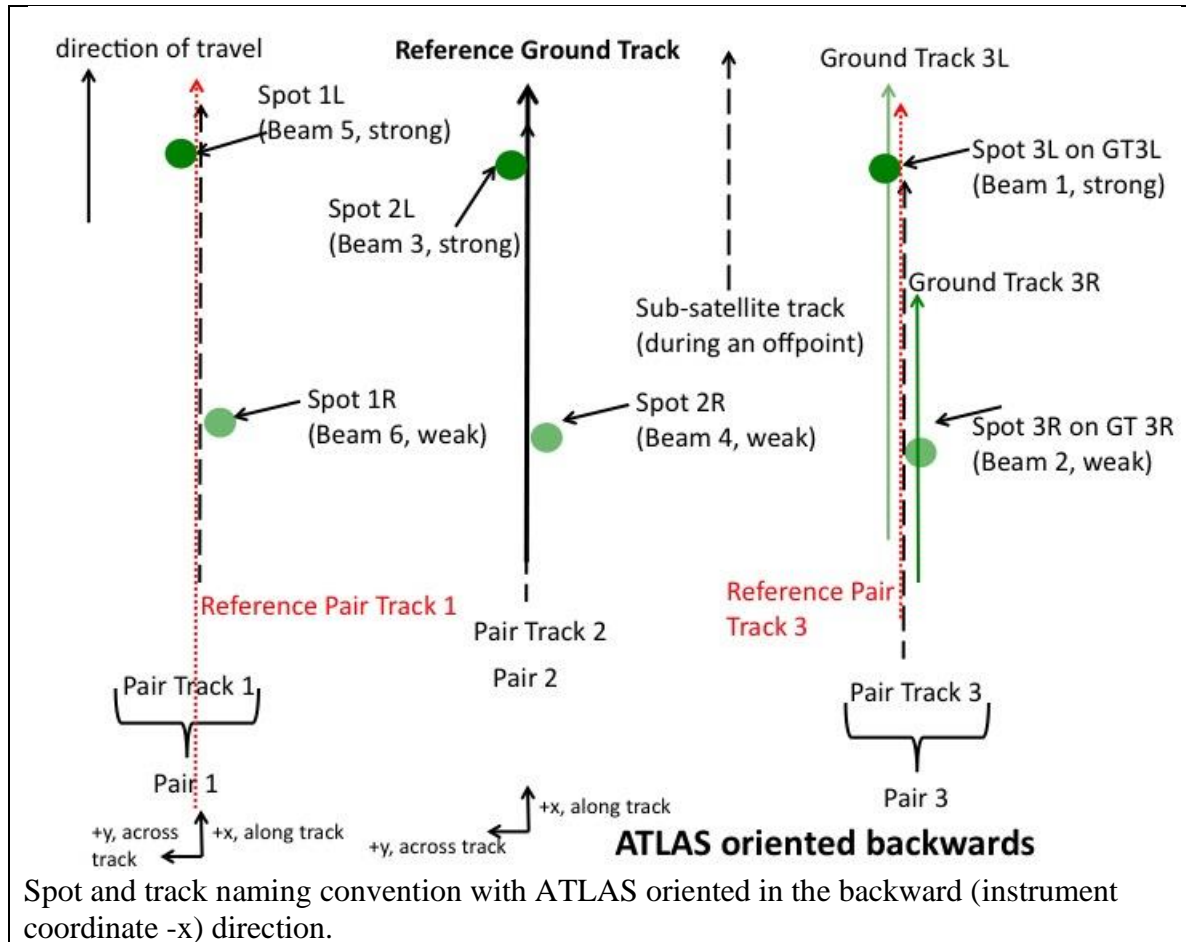
1393

Figure 6-3. Granule regions

Along-track product granule regions
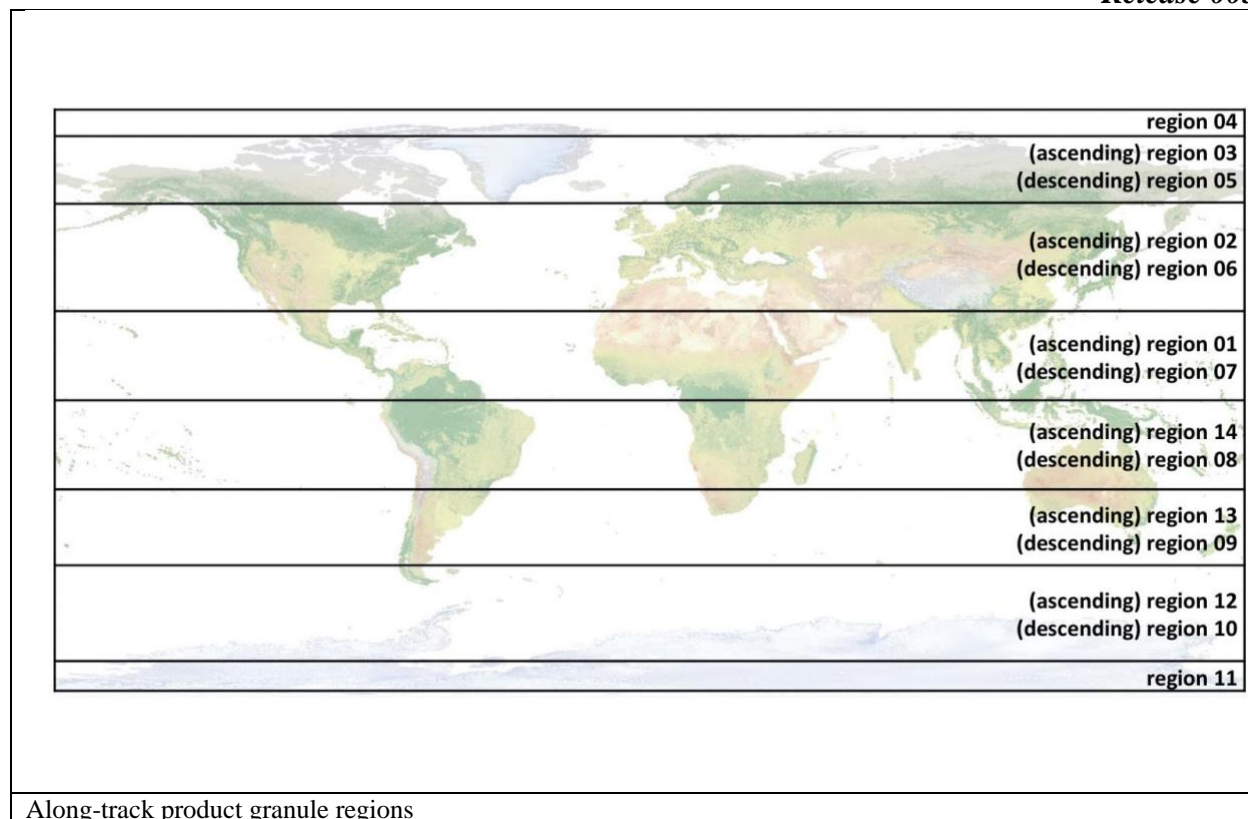
1394 **7.0   BROWSE PRODUCTS**

1395   For each ATL11 data file, there will be eight figures written to an associated browse file. Two of
1396   these figures are required and are located in the default group; default1 and default2. The browse
1397   filename has the same pattern as the data filename, namely,
1398   ATL11_ttttss_c1c2_rr_vVVV_BRW.h5, where tttt is the reference ground track, ss is the orbital
1399   segment, c1 is the first cycle of data in the file, c2 is the last cycle of data in the file, rr is the
1400   release and VVV is the version. Optionally, the figures can also be written to a pdf file.
1401
1402   Below is a discussion of the how the figures are made, with examples from the data file
1403   ATL11_009403_0307_02_vU07.h5. Note that the figure numbering in this section is distinct
1404   from that in the rest of the document; the figures shown here are labeled as they are in each
1405   browse-product file.
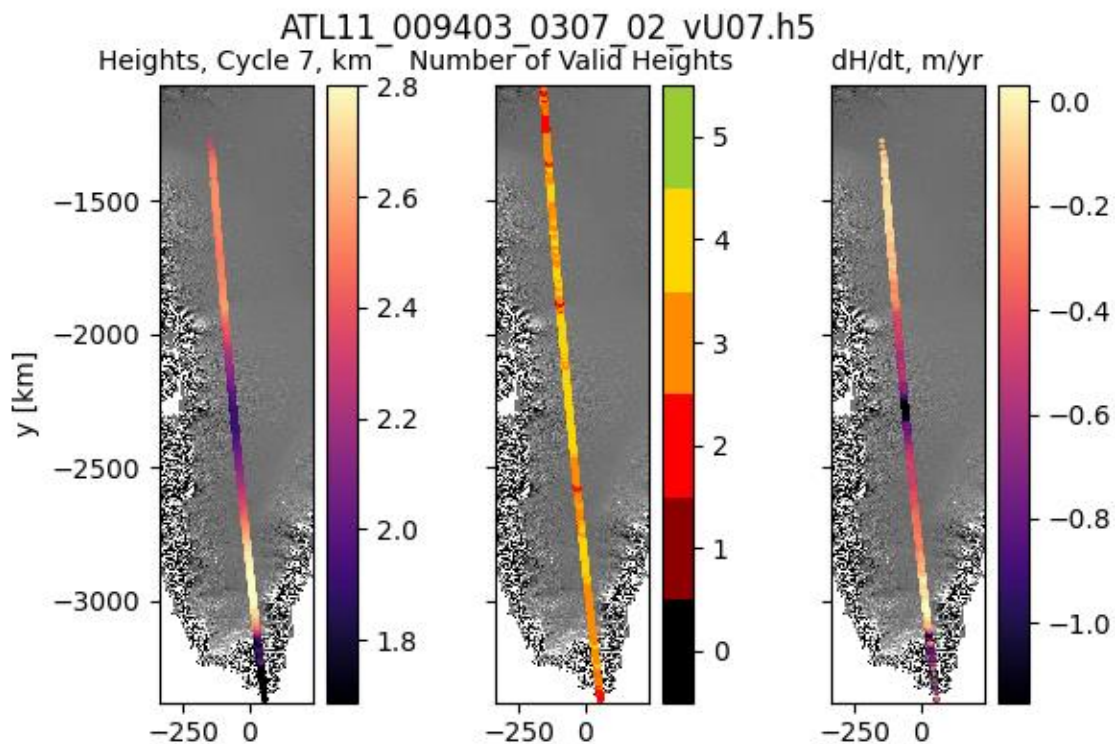1406
1407
1408

1409   Figure 1. Height data, in km, from cycle 7 (1st panel). Number of cycles with valid
height data (2nd panel). Change in height over time, in meters/year, cycle 7 from
cycle 3 (3rd panel). All overlaid on gradient of DEM. x, y in km. Maps are plotted in
a polar-stereographic projection with a central longitude of 45W and a standard
latitude of 70N.

1410

1411   The background for the three panels in Figure 1 is the gradient DEM in gray scale. It is shown in
1412   a polar-stereographic projection with a central longitude of 45W (0E) and a standard latitude of

1413   70N (71S), for the Northern (Southern) Hemisphere. The map is bounded by the extent of height
1414   data plus a buffer. ATL11 heights (/ptx/h_corr) from all pairs of the latest cycle with valid data,
1415   here cycle 7, are plotted in the first panel. The "magma" color map indicates the heights in km.
1416   The limits on the color bar are set with the python scipy.stat.scoreatpercentile method at 5% and
1417   95%. In the second panel are plotted the number of valid heights summed over all cycles at each
1418   location. The color bar extends to the total number of cycles in the data file. The change in height
1419   over time, dH/dt, is plotted in the third panel, in meters/year. dHdt is the change in height of the
1420   last cycle with valid data from the first cycle with valid data (/ptx/h_corr) divided by the
1421   associated times (/ptx/delta_time). Text of 'No Data' is printed in the panel if there is only one
1422   cycle with valid data, or if the first and last cycles with valid data have no common reference
1423   point numbers (/ptx/ref_pt). All plots are in x,y coordinates, in km. This figure is called
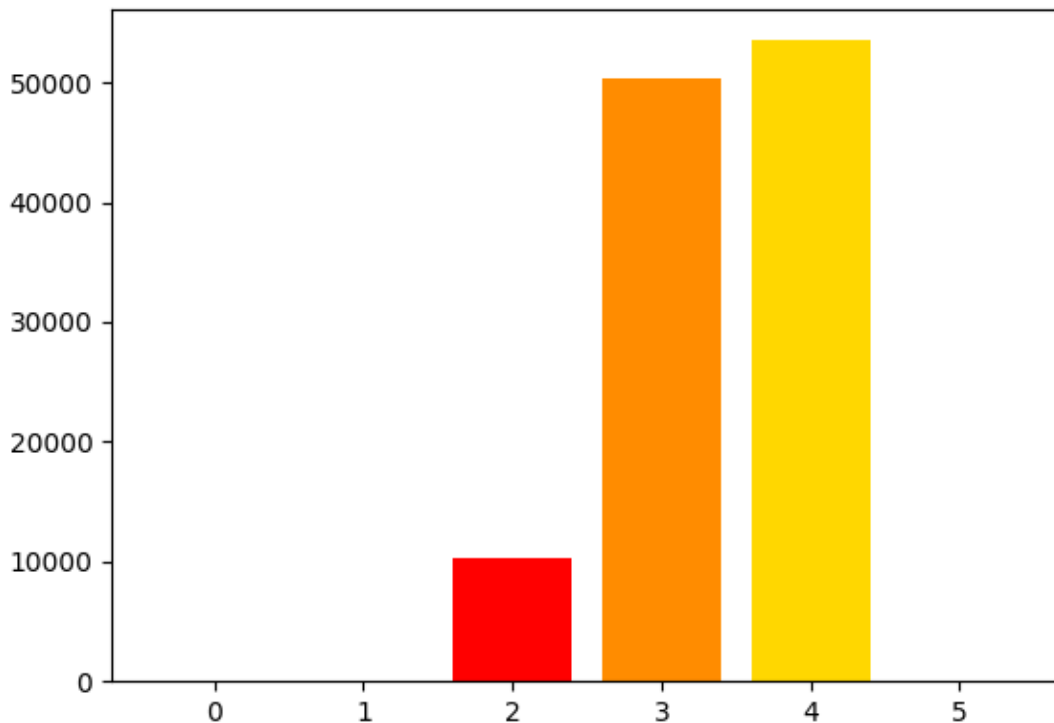1424   default/default1 in the BRW.h5 file.
1425

Figure 2. Histogram of number of cycles with valid height measurements, all beam
pairs.

1426
1427
1428   A histogram of the number of valid height measurements (/ptx/h_corr) is in Figure 2. Valid
1429   height data are summed across all cycles, for each reference point number (/ptx/ref_pt). The
1430   color scale is from zero to the total number of cycles in the data file and matches those in Figure
1431   1, 2nd panel. This figure is called validrepeats_hist in the BRW.h5 file.
1432
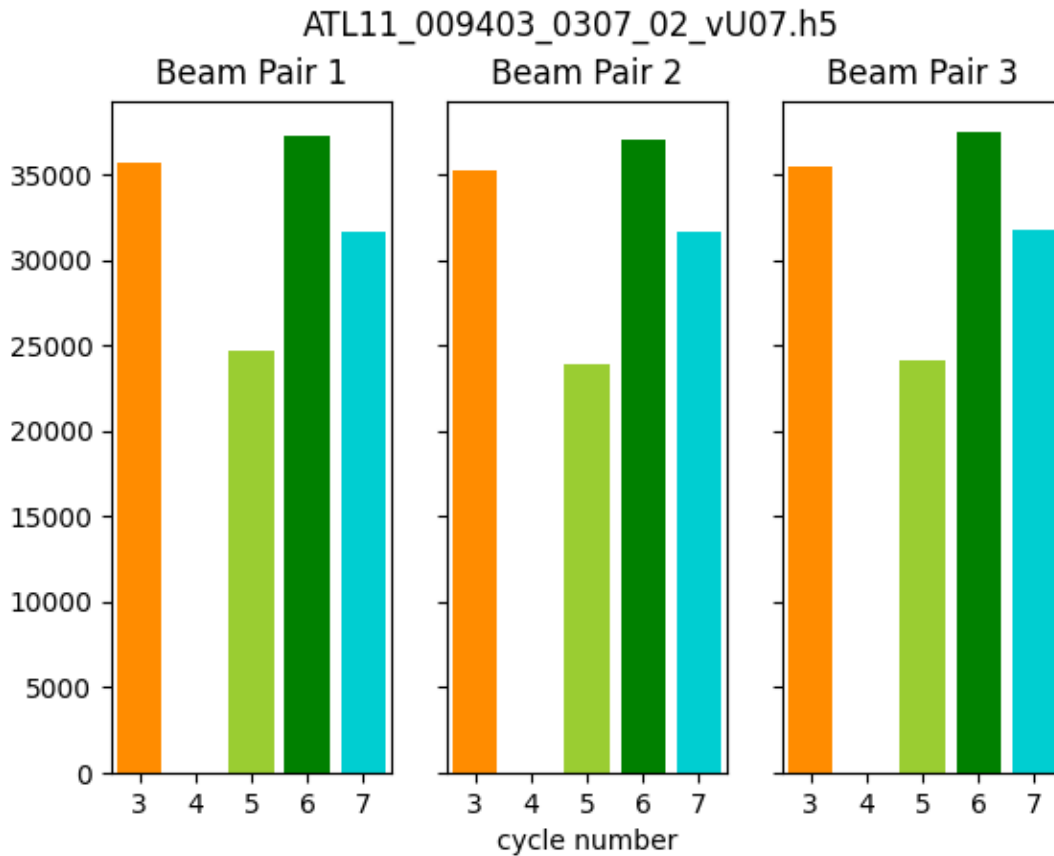
Figure 3. Number of valid height measurements from each beam pair.

1433
1434
1435   Histograms in Figure 3 show the number of valid heights (/ptx/h_corr) for each cycle, separated
1436   by beam pair. The cycle numbers are color coded. This figure is called default/default2 in the
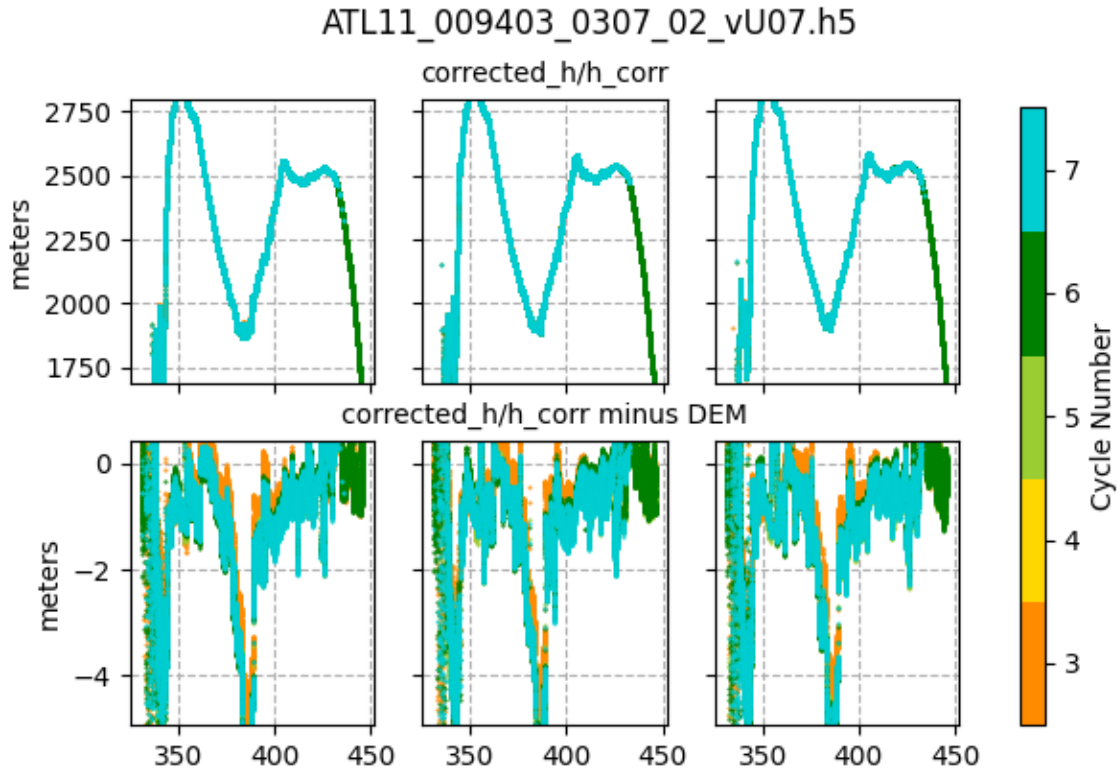1437   BRW.h5 file.
1438

49

Figure 4. Top row: Heights, in meters, plotted for each beam pair: 1 (left), 2 (center), 3 (right). Bottom row: Heights minus DEM, in meters. Y-axis limits are scores at 5% and 95%. Color coded by cycle number. Plotted against reference point number/1000.

1439

1440

1441 There are six panels in Figure 4, with two rows and three columns. In the top row are plotted the
1442 height measurements (/ptx/h_corr) for each beam pair, one pair per panel. In the bottom row are
1443 plotted the same height measurements minus the collocated DEM (ref_surf/dem_h) values, one
1444 pair per panel. The plots are color coded by cycle number, as in Figure 3. The heights are plotted
1445 versus reference point number (/ptx/ref_pt) divided by 1000 for a cleaner plot. The y-axis is in
1446 meters for both rows. The y-axis limits for the top and bottom rows are set separately, using the
1447 python scipy.stats.scoreatpercentile method with limits of 5% and 95% for heights and height
1448 differences, respectively. Text of 'No Data' is printed in a panel if there are no valid height data
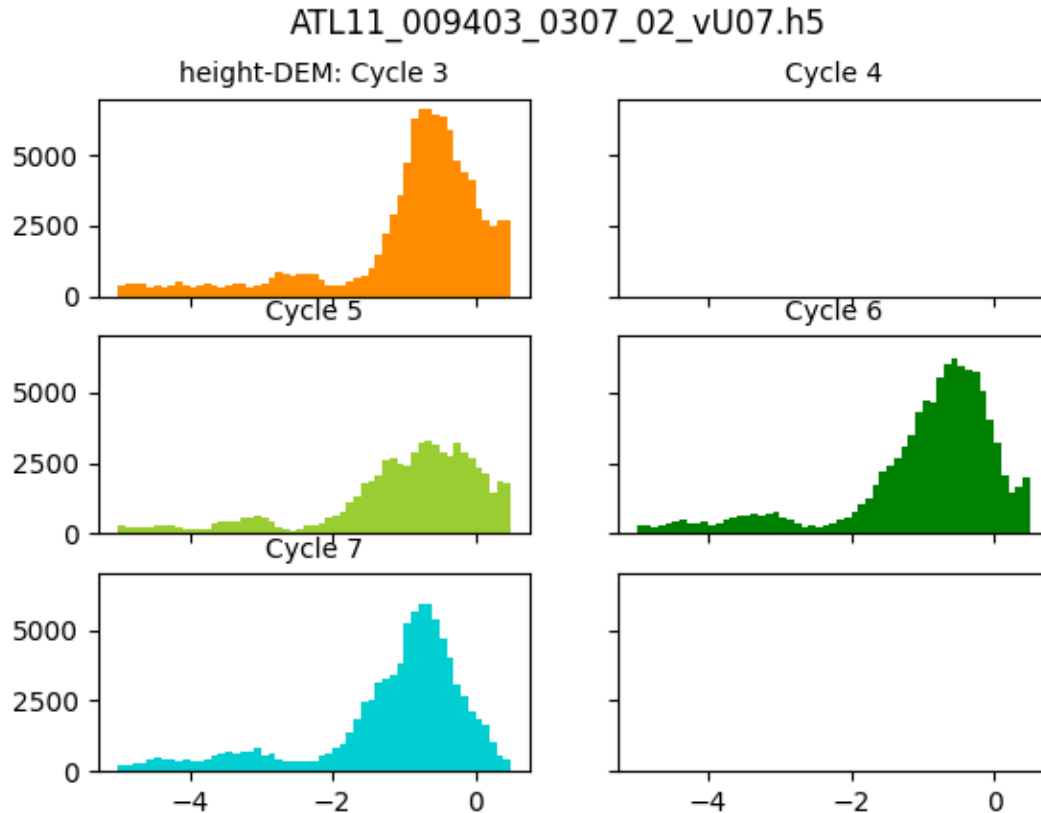1449 for that pair. This figure is called h_corr_h_corr-DEM in the BRW.h5 file.
1450

Figure 5. Histograms of heights minus DEM heights, in meters. One histogram per cycle, all beam pairs. X-axis limits are the scores at 5% and 95%.

1451
1452
1453 Figure 5 is associated with Figure 4. It is a multi-paneled figure, with the number of panels
1454 dependent on the number of cycles in the data file. Each panel is a histogram of the heights
1455 (/ptx/h_corr) minus collocated DEM heights (ref_surf/dem_h) color coded by cycle, the same as
1456 in Figures 3 and 4. The limits on the histograms are set using the python
1457 scipy.stats.scoreatpercentile method with limits of 5 and 95% for all cycles of data, the same
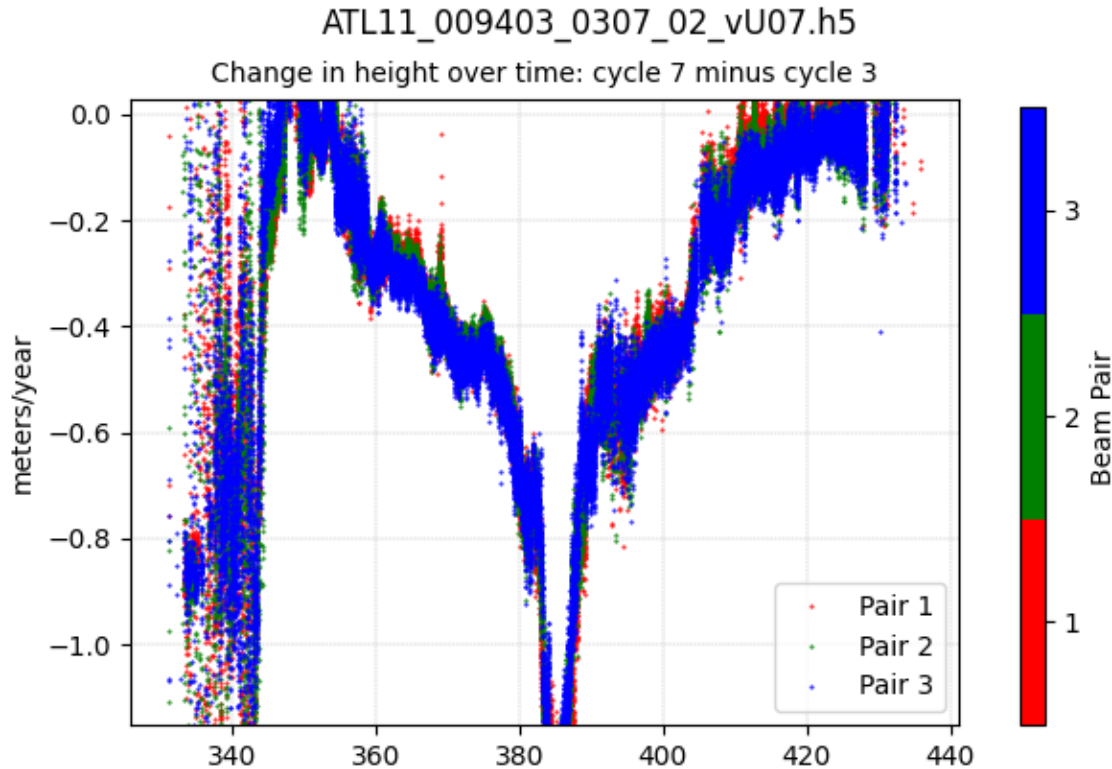1458 values used in Figure 4 bottom row. This figure is called h_corr-DEM_hist in the BRW.h5 file.
1459

51

Figure 6. Change in height over time, dH/dt, in meters/year. dH/dt is cycle 7 from cycle 3. Color coded by beam pair: 1 (red), 2 (green), 3 (blue). Y-axis limits are scores at 5% and 95%. Plotted against reference point number/1000.

1460
1461
1462   The changes in height with time, dH/dt, in meters/year are plotted in Figure 6. The calculation
1463   differences the first and last cycles with valid height data (/ptx/h_corr) divided by the associated
1464   time differences (/ptx/delta_time). The change in heights for pair 1 are in red, for pair 2 are in
1465   green and for pair 3 are in blue. The y-axis limits are set using the python
1466   scipy.stats.scoreatpercentile method with limits of 5% and 95%. The x-axis is reference point
1467   number (/ptx/ref_pt) divided by 1000 for a cleaner plot. Text of 'No Data' is printed in the panel
1468   if there is only one cycle with valid data, or if the first and last cycles with valid data have no
1469   common reference point numbers. This figure is called dHdt in the BRW.h5 file.
1470
1471

1472   **Glossary/Acronyms**

ASAS	ATLAS Science Algorithm Software
ATBD	Algorithm Theoretical Basis Document
ATLAS	ATLAS Advance Topographic Laser Altimeter System
CDF	Cumulative Distribution Function
DEM	Digital Elevation Model
GSFC	Goddard Space Flight Center
GTs	Ground Tracks
ICESat-2	Ice, Cloud, and Land Elevation Satellite-2
IKR	I Know, Right?
MABEL	Multiple altimeter Beam Experimental Lidar
MIS	Management Information System
NASA	National Aeronautics and Space Administration
PE	Photon Event
POD	Precision Orbit Determination
PPD	Precision Pointing Determination
PRD	Precise Range Determination
PSO	ICESat-2 Project Science Office
PTs	Pair Tracks
RDE	Robust Dispersion Estimate
RGT	Reference Ground Track
RMS	Root Mean Square
RPTs	Reference Pair Tracks
RT	Real Time
SCoRe	Signature Controlled Request
SIPS	ICESat-2 Science Investigator-led Processing System
TLDR	Too Long, Didn't Read
TBD	To Be Determined

53

1473 **References**

1474   Brunt, K.M., H.A. Fricker and L. Padman 2011. Analysis of ice plains of the Filchner-Ronne Ice
1475   Shelf, Antarctica, using ICESat laser altimetry. *Journal of Glaciology*, **57**(205): 965-975.

1476   Fricker, H.A., T. Scambos, R. Bindschadler and L. Padman 2007. An active subglacial water
1477   system in West Antarctica mapped from space. *Science*, **315**(5818): 1544-1548.

1478   Schenk, T. and B. Csatho 2012. A New Methodology for Detecting Ice Sheet Surface Elevation
1479   Changes From Laser Altimetry Data. *Ieee Transactions on Geoscience and Remote Sensing*,
1480   **50**(9): 3302-3316.

1481   Smith, B., H.A. Fricker, N. Holschuh, A.S. Gardner, S. Adusumilli, K.M. Brunt, B. Csatho, K.
1482   Harbeck, A. Huth, T. Neumann, J. Nilsson and M.R. Siegfried 2019a. Land ice height-retrieval
1483   algorithm for NASA's ICESat-2 photon-counting laser altimeter. *Remote Sensing of*
1484   *Environment*: 111352.

1485   Smith, B.E., H.A. Fricker, I.R. Joughin and S. Tulaczyk 2009. An inventory of active subglacial
1486   lakes in Antarctica detected by ICESat (2003-2008). *Journal of Glaciology*, **55**(192): 573-595.

1487   Smith, B.E., D. Hancock, K. Harbeck, L. Roberts, T. Neumann, K. Brunt, H. Fricker, A.
1488   Gardner, M. Siegfried, S. Adusumilli, B. Csatho, N. Holschuh, J. Nilsson and F. Paolo 2019b.
1489   Algorithm Theoretical Basis Document for Land-Ice Along-track Product (ATL06). Goddard
1490   Space Flight Center.

1491